Repeated and Sudden Reversals of Dipole Field Generated by A Spherical Dynamo Action

Jinghong LI

DOCTOR OF PHILOSOPHY

Department of Fusion Science
School of Mathematical and Physical Science
The Graduate University for Advanced Studies

2001 (School Year)

Abstract

The magnetic fields of planetary and astrophysical bodies, such as the Sun and the Earth, are believed to be generated by a dynamo action in a moving electrically conducting fluid. The mathematical problem describing the generation of magnetic fields by self-inductive action in an electrically conducting fluid is called the dynamo problem. The dynamo process converts the mechanical energy of electrically conducting fluid into the magnetic energy and dissipates it in the form of ohmic heat.

On the surface of the Earth and above, the dipole component of the Earth's magnetic field is dominant, and its dipole axis is ever changing. The Earth's magnetic field has existed on average at roughly its present strength in its history and is constantly changing. Its polarity has reversed many hundreds of times at irregular intervals during the Earth's history.

Recent accelerated development in supercomputer technology makes it possible to achieve three-dimensional MHD dynamo simulations which self-consistently solve for fluid flow and magnetic field in three dimensions. Significant progress in recent years is the development of numerical simulation of convection-driven dynamo in rotating spherical shells that achieve self-sustaining dynamo actions. Some models have realized dominant dipole fields outside the shells. Several numerical models of convective dynamos even successfully have thus far reproduced some of the basic properties of the Earth's magnetic field.

Reversal of the magnetic field is one interesting and challenging problem in MHD theory. Some authors have already succeeded in demonstration of magnetic field reversal by three dimensional dynamo simulations. In particular, Glatzmaier and Roberts presented the first numerical simulation of a complete field reversal. The first numerical simulation of dynamical flip-flop type transition of the magnetic energy level and its association with the reversals of the dipole and octupole field polarity were obtained by Kageyama and Sato. Later, Glatzmaier et al. showed that more frequent reversals occur in their simulation by changing the core-mantle boundary condition. Coe et al. described the evolution of the morphology and/or spectral energy of simulated magnetic fields during reversals. However, physical understanding of the mechanism of magnetic polarity reversals is yet

veiled.

The mechanism of the magnetic field reversal still remains one of the challenging phenomena in MHD dynamo theory. To understand the mechanism by which the polarity of the magnetic field is reversed in MHD dynamo, a very long time numerical simulation is carried out by using Kageyama-Sato MHD dynamo model in this thesis. The simulation results show that the generated magnetic field is dipole dominated in most simulation time and reverses its polarity. The reversals of magnetic field occur repeatedly and irregularly. The magnetic field reversal appears to occur without any regular rule. It does reverse suddenly and the reversal does continue endlessly. As a whole, it is unlikely that the existence of one polarity predominates over the other.

The thermal convection in the rapidly rotating spherical shell is caused by gravity and the temperature difference between inner and outer cores, which takes the form of columnar cells which are parallel to the rotation axis. The magnetic field is generated and amplified through the fluid convection motion which stretches and twists the magnetic field lines. The magnetic field structure inside the spherical shell is very complicated. Generally, the magnetic field lines spiral around the convection columns. Interestingly, in the whole evolution, the total magnetic and kinetic energies exhibit a flip-flop alternation between a high energy state and a low energy state. The different energy states correspond to different magnetic field configurations and convection patterns. In low energy states, the convection columns drift westwards and keep almost unchanged structures. The convection motion in high energy states exhibits the basic columnar structure, but nevertheless it is time-dependent.

The magnetic field reversal is studied in details. From the analysis of the time evolution of magnetic field, we obtain the necessary conditions for the occurrence of a dipole reversal: (1) the system is in a high energy state, (2) the high energy state lasts for a certain period, (3) the quadrupole mode is on the average in a growing phase, and (4) the magnitude of the quadrupole mode exceeds that of the dipole mode on the outer boundary.

The magnetic field is generated by the convection motion of the electrically conducting fluid in the sphere shell. So the magnetic field pattern is strongly correlated with the fluid flow. In low energy states, the axial component of fluid velocity in the equatorial plane (i.e., trans-equatorial flow) is very weak. The convection motion is symmetric around the equatorial plane. While in high energy states, the trans-equatorial component of fluid velocity in the equatorial plane is very strong. The north-south symmetry around the equatorial plane is broken. The existence of the trans-equatorial flows in high energy states suggest that there is a strong interaction of fluid motion between the northern hemisphere and the southern hemispheres. This strong interaction of fluid flow is likely to initiate a reversal of magnetic field.

The most important and crucial discovery of this thesis is the generation of trans-equatorial flows in a spherical system that make the convection pattern vulnerable and the whole system marginally stable, the reversal of the dipole magnetic field thereby being triggered occasionally and unexpectedly.

The effects of electrical resistivity and the temperature difference between the inner and outer boundaries to the magnetic field reversals are also analyzed. We find that the electrical resistivity is one of important physical parameters to the generation and reversal of the magnetic field.

To sum up, in our numerical simulations of MHD dynamo, we have observed repeated and sudden magnetic field reversals, and obtained the conditions for magnetic field reversal. Furthermore, we have studied the physical mechanism of the magnetic field reversals and come to the conclusion that the break of the north-south symmetry around the equatorial plane of convection motion must be the primary cause of the magnetic field reversal.

Contents

Chapter 1

Introduction

1.1 Overview

It is well known that many planetary and astrophysical bodies, such as the Sun and the Earth, possess magnetic fields. From the spectral lines of the solar spectrum split by Zeeman effect, it is inferred that the sunspots are the seat of strong magnetic fields. The magnetic polarity of sunspot pairs in either hemisphere is observed to reverse in 11 years, so the magnetic cycle of the Sun has a period of 22 years. The Earth's magnetic field is dipole-dominated and varies slowly with time [1, 2]. Its dipole axis is tilted at about 11° (or it makes an angle of about 11° with the Earth's rotation axis) at the present time. The Earth was found to possess magnetic field several thousands years ago. Besides the Sun and the Earth, the other planets in the solar system, Mercury, Jupiter, Saturn, Uranus, and Neptune, also have substantial magnetic field [3, 4], which are confirmed mostly from the observation of spacecrafts. At the present time, Mercury, like the Earth, appears to have a significant dipole magnetic field. The magnetic field of Jupiter is large in magnitude and its dipole axis is nearly parallel to its rotation axis. The Saturn possesses the most unusual magnetic field. Its magnetic field appears to be symmetric with respect to the rotation axis. The magnetic fields of Uranus and Neptune are very much alike, but quite different from those of Jupiter, Saturn and Earth. Both of them possess global magnetic fields for which the dipole magnetic axis are offset from the rotation axis and their magnetic centers are spatially displaced by a significant amount from the centers of the planets. Magnetic fields are also found in other stars, planets and galaxies.

Obviously, origins of planetary magnetic fields can not be explained in terms of permanent magnetization, because the temperatures of their interiors are well above the

Curie temperature of all known materials, at which ferromagnetic materials lose their magnetization. Larmor[5] was the first to suggest the dynamo process as an explanation for the magnetic field in sunspots. Now, it is widely accepted that these magnetic fields are to be generated by the dynamo action in a moving electrically conducting fluid[6, 7, 8, 9, 10, 11, 12].

Interpretation of these magnetic fields requires knowledges of the planets' interior structures. All of these magnetic planets share the same essential features: They are rotating rapidly and have a large core of electrically conducting liquid metal in the shape of a sphere or spherical shell. The maintenance of currents in planetary interiors requires active dynamos, since the Ohmic decay times are short compared to the age of the solar system.

The mathematical problem describing the generation of magnetic fields by self-inductive action in an electrically conducting fluid is called the dynamo problem. The dynamo process converts the mechanical energy of electrically conducting fluid into the magnetic energy and dissipates it in the form of ohmic heat.

Much numerical simulation effort has been done with the aid of supercomputer to achieve three-dimensional magnetohydrodynamics (MHD) dynamo simulations which simultaneously solve for fluid flow and magnetic field in three dimensions. There has been significant progress in the numerical simulations of convection-driven dynamos. Several numerical models of convective dynamos in spherical shells successfully reproduce some of the basic properties of the Earth's magnetic field, such as reversals of the generated magnetic field polarity, which is one phenomenon of self-organization created in an open nonlinear system[13].

1.2 The Earth's Magnetic Field

The Earth provides us with a good example to study the dynamo problem, because the Earth's magnetic field has exhibited a wide range of space-time variability during its historical times. We have direct measurement of the Earth's magnetic field strength and direction for the past few hundred years. By indirect measurements, or measuring the direction and intensity of magnetism in rocks of different ages, we can obtain the information of the Earth's magnetic field that go back some 3×10^9 years[1, 2].

The information of the Earth's magnetic field is very helpful for understanding the dynamo action happened in the outer core of the Earth. The deep understanding of the

Earth's magnetic field and its interior will promote and enrich the development of the MHD dynamo theory.

1.2.1 The Earth's Interior Structure

The Earth is an almost spherical object (see Fig. 1.1). Its internal structure shows primary layered structure. The innermost part of the core (red) is now solid, whereas the intermediate part (orange) is electrically conducting fluid which consists of molten metal, probably iron with a weak admixture of lighter elements, sulphur, carbon or silicon. The inner core is most probably an alloy of iron and nickel, presumably formed by slow crystallization from the outer core.

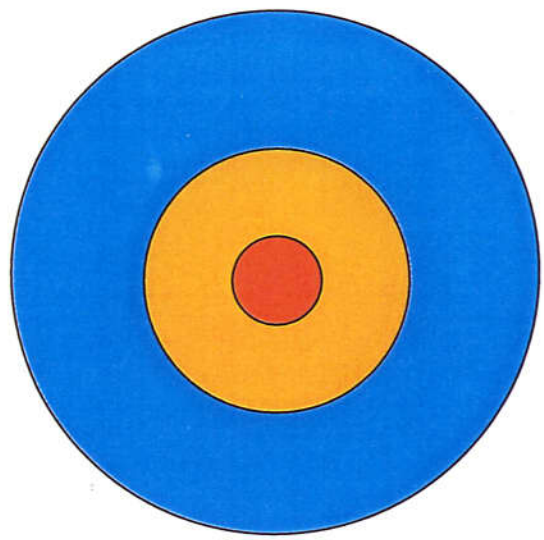

Figure 1.1: A model of the Earth's interior structure. The red part is solid inner core, the orange part fluid outer core (dynamo action region), and the blue part rocky mantle.

1.2.2 History of the Earth's Magnetic Field

The Earth's magnetic field has existed on average at roughly its present strength in its whole history and is constantly changing[2, 14, 15, 16, 17]. On the surface of the Earth and above, the dipole component of the Earth's magnetic field is dominant, its dipole axis is always changing. This is an important property of the Earth's magnetic field. The dynamo action happens in the outer core of the Earth.

The magnetic field of the Earth shows spatial distribution. Besides dipole component, the Earth's magnetic field possesses other components (called non-dipole field), which can be obtained by using the spherical harmonic analysis method [18]. Apart from its spatial variation, the Earth's magnetic field also varies with time. The magnetic field pattern shows drift motion. The drift is latitude dependent and irregular. Westward, standing, eastward and meridional motions of the non-dipole field have all been claimed to be dominant in the historical record [2].

In summary, the Earth's magnetic field have the following two basic properties:

1. The dipole component of the Earth's magnetic field is dominant.
2. The non-dipole field pattern of the Earth's magnetic field is drifting.

1.2.3 Reversals of the Earth's Magnetic Field

The magnetic field of the Earth is dipole dominated and is constantly changing. It not only changes its intensity, but also reverses its polarity. In fact, the reversals of the Earth's magnetic field were originally found in lava flows whose magnetizations were roughly opposed to that of the present Earth's magnetic field[19, 20].

The Earth magnetic field has reversed its polarity many hundreds of times at irregular intervals during the Earth's history[1, 2, 14]. On a geological timescale, a polarity transition takes place so quickly that it is difficult to find the paleomagnetic evidence that have preserved a complete and accurate record. The duration of a reversal is generally thought to be between 1000 and 6000 years, during which time the average intensity of the field at Earth's surface is estimated to decrease to about a quarter of its usual value.

Among the observation data of the Earth's magnetic field reversal, the following three results are very important for the magnetic field reversal mechanism study in MHD dynamo.

1. The occurrence of the Earth's magnetic field reversals appears to be time-dependent.
2. The reversal duration are relatively short compared with the constant polarity intervals between reversals.
3. The normal and reverse polarities of the Earth's magnetic field are equivalent quasi-equilibrium states.

1.3 Dynamo Problem

The dynamo problem is a branch of magnetohydrodynamics [21, 22]. It describes the generation of magnetic fields by self-inductive action in an electrically conducting fluid. In mathematics, it involves the solution of a highly complicated system of coupled partial differential equations: the electrodynamic equations for fields, hydrodynamic equations for fluid motion, and thermodynamic equations for materials.

In dynamo theory, the magnetic induction equation is one of the most important equations.

1.3.1 Magnetic Induction Equation

Under the MHD approximation, in which the displacement current is neglected, the fundamental equations describing electric and magnetic fields are pre-Maxwell's equations:

$$\nabla \cdot \mathbf{D} = \theta \tag{1.1}$$

$$\nabla \cdot \mathbf{B} = 0 \tag{1.2}$$

$$\nabla \times \mathbf{E} = -\frac{\partial \mathbf{B}}{\partial t} \tag{1.3}$$

$$\nabla \times \mathbf{H} = \mathbf{J} \tag{1.4}$$

where θ is the free charge density, $\mathbf{J}$ is the electric current.

The electric displacement $\mathbf{D}$, the electric field $\mathbf{E}$, the magnetic induction $\mathbf{B}$ and the magnetic field $\mathbf{H}$ are related through material equations:

$$\mathbf{D} = \epsilon \mathbf{E} \tag{1.5}$$

$$\mathbf{B} = \mu \mathbf{H} \tag{1.6}$$

where ϵ is the permittivity, and μ is the permeability.

Combining with the generalized Ohm's law

$$\mathbf{J} = \sigma(\mathbf{E} + \mathbf{v} \times \mathbf{B}) \tag{1.7}$$

we can obtain the magnetic induction equation as following:

$$\frac{\partial \mathbf{B}}{\partial t} = \nabla \times (\mathbf{v} \times \mathbf{B}) + \eta \nabla^2 \mathbf{B} \tag{1.8}$$

where

$$\eta = (\mu\sigma)^{-1} \tag{1.9}$$

is known as the magnetic diffusivity, σ is the electrical conductivity.

In dynamo problem, generally we study how the magnetic field is generated by the dynamo action in a moving electrically conducting fluid that does not possess permanent magnetic moment in the absent of external magnetic field. In this case, the permeability is that of free space. So the magnetic diffusivity (It is called the electrical resistivity later in this thesis.) is

$$\eta = (\mu_0\sigma)^{-1} \tag{1.10}$$

In the magnetic induction equation, for the magnetic field $\mathbf{B}$, the source term is the induction term, $\nabla \times (\mathbf{v} \times \mathbf{B})$, and the lose term is the diffusion term, $\eta\nabla^2\mathbf{B}$. Evidently the magnetic Reynolds number, the ration of the induction term and the diffusion term in the magnetic induction equation, is very important for dynamo action. The condition for dynamo action in general requires that the magnetic Reynolds number exceeds a certain finite value.

1.3.2 Kinematic Dynamo

Generally, dynamo theory is divided into two parts: Kinematic theory and MHD dynamo. Kinematic theory supposes that the velocity field is given, and seeks self-excited solutions of the induction equation, or a solution of magnetic field which does not decay to zero as time goes to infinity. Its central task is to determine for what fluid field self-excited solutions arise. MHD dynamo theory attempts to determine both magnetic field and fluid velocity field jointly by solving the full MHD equations for some given power source, such as thermal buoyancy.

Kinematic dynamo theory has been intensively studied because kinematic dynamo problem is linear in the magnetic field. It has provided great insights into basic dynamo process, and plays very important role in the development of dynamo theory[6, 23], especially in establishing some necessary conditions for dynamo action to occur and anti-dynamo theorems, such as the well-known Cowling's anti-dynamo theorem[21, 24], one of the first results in dynamo theory, which states that a magnetic field symmetric about an axis cannot be maintained by a symmetric motion.

1.3.3 Magnetohydrodynamic Dynamo

The kinematic dynamo problem describes the dynamo process in its initial stages, when a particular mode among the small random magnetic disturbance that permeate the universe becomes amplified by dynamo action. When the amplitude of the magnetic field reaches such a value that the Lorentz force in the equation of motion is no longer negligible, the magnetohydrodynamic dynamo problem must be solved.

Although the Lorentz force is undoubtedly important, a knowledge of the dynamics without the Lorentz force is a prerequisite for understanding the dynamo process, since the latter represents an instability of the state without a magnetic field. Knowledge of the general behavior of thermal convection in rapidly rotating systems is crucial to understand dynamo action. A standard formulation of the problem has been given by Chandrasekhar[25], and an asymptotic linear analysis for the limit of rapid rotation has been developed by Roberts[26] and Busse[27].

In MHD dynamo theory, strong interaction of fluid motion and magnetic field, especially the interaction between the Coriolis and Lorentz forces, and strong nonlinearity of the MHD dynamo equations make it difficult to study the dynamo problem analytically. While the fluid motions driven by convection generate and sustain magnetic fields by MHD dynamo processes, the pattern and strength of the convective motion that control dynamo action are critically influenced by the combined and inseparable effects of rotation, magnetic fields, and spherical geometry [28, 29].

To solve the full three-dimensional MHD dynamo problem at sufficient resolution and driven strongly enough for magnetic field generation requires huge computational resources, so it is clearly not possible to undertake the exploration of parameter space required to gain a full understanding of the system. Complementary, simpler calculations are still required. There has been enormous progress in recent years through studying such a model problems.

The magnetic field reversal is not an isolated phenomenon. The Earth's magnetic field has reversed its polarity many hundreds of times. The Sun also has a general magnetic field that appears to reverse its polarity frequently with a period of 11-year. The magnetic field reversal should be an universal phenomenon in MHD dynamo problem.

1.3.4 Progresses in MHD Dynamo Simulation

Gilman and Miller realized the first spherical MHD simulations of the solar dynamo model in the early 1980s[30, 31].

Recently, the high speed development in supercomputer technology makes it possible to achieve three-dimensional MHD dynamo simulations which simultaneously solve for fluid flow and magnetic field in three dimensions. There has been significant progress in the numerical simulations of convection-driven dynamos.

Several numerical models of convective dynamos in spherical shells successfully reproduce some of the basic properties of the Earth's magnetic field, although computational limitations currently prevent these calculations from reaching the Earth's physical conditions. Numerical models of the geodynamo developed by Glatzmaier and Roberts [32, 33, 34, 35, 36] and Kuang and Bloxham [37] produced results bearing resemblance to the present geomagnetic field with strong dipolar component and its secular variation. The first Earth-like magnetic field was generated by Glatzmaier and Roberts [32, 33], who made the effects of viscosity and inertia as small as possible. Kuang and Bloxham [37, 38] also reported that their calculated magnetic field is very similar in structure and intensity to the Earth's field and their dynamo solution operates in an Earth-like dynamical regime. They reduced the influences of viscous forces at the boundaries by using stress-free boundary conditions, rather than the more common used no-slip conditions. In addition, some parameter studies of geodynamo numerical modelling were also made[39, 40].

Besides many efforts that have been directed towards simulations of the Earth dynamo, other numerical simulations have been directed towards simpler configurations in order to promote a deeper understanding of convection-driven dynamos[41, 42, 43, 44, 45, 46, 47, 48, 49].

Hollerbach and Jones[50] studied the influence of the Earth's inner core on the Earth's magnetic field and found that the rapid advective fluctuation in the outer core is effectively averaged out by the inner core, producing a relatively stable external dipole field. Sakuraba and Kono[51] also studied the effect of the inner core on the dynamo process and suggested that the Earth's magnetic field may be stabilized as the inner core grows, even though the total energy input is the same.

Recently Grote et al. find that quadrupolar dynamos become preferred in their numerical simulation model[52], while other dynamo simulations usually are the types of dipole-dominated magnetic field.

The reversal of the magnetic field is one interesting and challenging problem in MHD theory. Some progresses on the magnetic field reversal have been made in three dimensional dynamo simulations. In particular, Glatzmaier and Roberts presented the first numerical simulation of a complete field reversal[33]. The first numerical simulation of dynamical flip-flop type transition of the magnetic energy level and its association with the reversals of the dipole and octupole field polarity was obtained in the previous simulation[44, 53] of Kageyama-Sato model[41, 42]. Later, Glatzmaier et al. [36] show that more frequent reversals occur in their simulation by changing the core-mantle boundary condition. Coe et al. [54] described the evolution of the morphology and/or spectral energy of simulated magnetic fields during reversals. Sarson and Jones [55] and Sarson[56] have made an argument on the important of non-axisymmetric poloidal flow on the reversal. However physical understanding of the mechanism of magnetic polarity reversals is yet veiled.

The mechanism of the magnetic field reversal still remains one of the challenging phenomena in MHD dynamo theory.

1.4 Laboratory Dynamo

Considerable progresses in MHD dynamo theory and simulations are achieved. Meanwhile, some experimental efforts to realize dynamo action in laboratory by using flowing liquid metals are going on in Europe and North America[57, 58, 59, 60, 61, 62]. Due to the large dimensions of the length scale and/or the velocity scale which are necessary for dynamo action to occur [22], until very recently, the laboratory dynamo shows some exciting results in the Riga Dynamo Facility[59, 62].

Usually liquid sodium is used for the experiment of laboratory dynamo. Sodium is much more reactive as a liquid than as a solid; it will burn easily in air, and its reaction with water can be explosive. It is this safety problems that makes the laboratory dynamo in laboratory very difficult to work. After years of hard working, magnetic field self-excitation in a spiraling liquid metal flow produced by a propeller was realized, in which a dynamo eigenmode slowly growing in time was observed for the first time[59]. Recently the saturation of the generated magnetic field has been realized[62].

The recent experiments of laboratory dynamo are indeed exciting. It is no doubt that these developments on the laboratory dynamos will lead to a deeper understanding of the origin of magnetic fields in planets and in stars.

However, there is still a long way to go for the laboratory dynamo, because the laboratory dynamo at present stage is different from those ones happened in the planets, in which dynamo actions occur in rotating fluid spheres or spherical shells and the fluid flowing are driven by some sources such as convection motions.

1.5 Motivation and Outline

The mechanism of magnetic field reversal is one of the most difficult problems in MHD dynamo. Until 1995, the first numerical simulation of a complete field reversal was realized[33]. Later, in 1999, the reversals of the dipole and octupole field polarity[44], which are accompanied by dynamical flip-flop type transition of the magnetic energy level, were observed in Kageyama-Sato convection-driven dynamo model. However, only one dipole magnetic reversal occurred in this simulation.

Under this situation, this work started. The main goal of this work is to understand the mechanism of the magnetic field reversal in MHD dynamo, namely the condition of magnetic field reversal, and the relationship of the reversals and the fluid convection motion. To obtain a number of reversals is important and necessary for understanding the physics of magnetic field reversal.

In order to study the mechanism of the magnetic field reversal, we must obtain the magnetic field reversals in the simulation. At the beginning of this work, the main purpose was to find out the parameter region in which the magnetic field reversals can occur. At that time, we even did not make sure if we could obtain a number of reversals. Starting from the magnetic induction equation (1.8) and considering the hydrodynamics of the convection of fluid, we thought that the electrical resistivity and the temperature difference between of the inner boundary and the outer boundary maybe affect the behavior of the magnetic field polarity. The followings are the reasons for these choices. Generally, the magnetic Reynolds number depends on the electrical resistivity of electrically conducting fluid. It should be larger enough to maintain the dynamo action. The change of electrical resistivity will influence the behavior of the magnetic field. For the convection-driven dynamo, the strength of the thermal driving depends on the temperature difference of inner and outer boundaries. This temperature difference can control the thermal convection state. These choices are proved to be correct ones in our numerical simulation.

This thesis is organized in the following way:

In Chapter 2, we describe the simulation model, or Kageyama-Sato dynamo model, the

corresponding three-dimensional MHD equations, boundary conditions, initial conditions, and numerical method.

In Chapter 3, we give a brief description of the simulation parameter sets used in MHD dynamo simulations, and an overview of the simulation results.

In Chapter 4, a long time simulation result is analyzed in detail. In this simulation, the reversals of magnetic field occur repeatedly and irregularly. The conditions of the magnetic field reversal are clarified.

In Chapter 5, we analyze the structure of the convection motion and the structure of the magnetic field, then give a conclusion about the reversal mechanism that break of north-south symmetry of fluid convection motion will lead to the magnetic field reversal.

In Chapter 6, some interpretations on the interaction of the convection motion and magnetic field at high energy states and low energy states in the standard simulation result are presented.

In Chapter 7, the effects of electrical resistivity and the temperature difference between the inner and outer boundary are discussed.

Finally, we give some conclusions and make a summary in Chapter 8.

Chapter 2

Simulation Model

In this chapter we shall give an introduction to Kageyama-Sato MHD dynamo simulation model[41, 42] and the related basic equations, boundary conditions, and initial conditions. The primitive purpose of Kageyama-Sato model is to investigate the fundamental process of the MHD dynamo, so a simple simulation model is used. This model is successful in explaining the magnetic field formation and the generation mechanism of a dipole field[41, 42, 43]. A magnetic field reversal was also observed in previous work[44, 53] by using this model.

2.1 Simulation Geometry

In Kageyama-Sato model[41, 42], we consider three-dimensional, time-dependent, thermal convection and magnetic field generation in an electrically conducting compressible spherical fluid shell, which rotates with constant angular velocity Ω. The inner boundary of radius r_i and outer boundary of radius r_o of the spherical shell are treated as co-rotating solid surfaces. The simulation geometry of Kageyama-Sato model is shown in Figure 2.1.

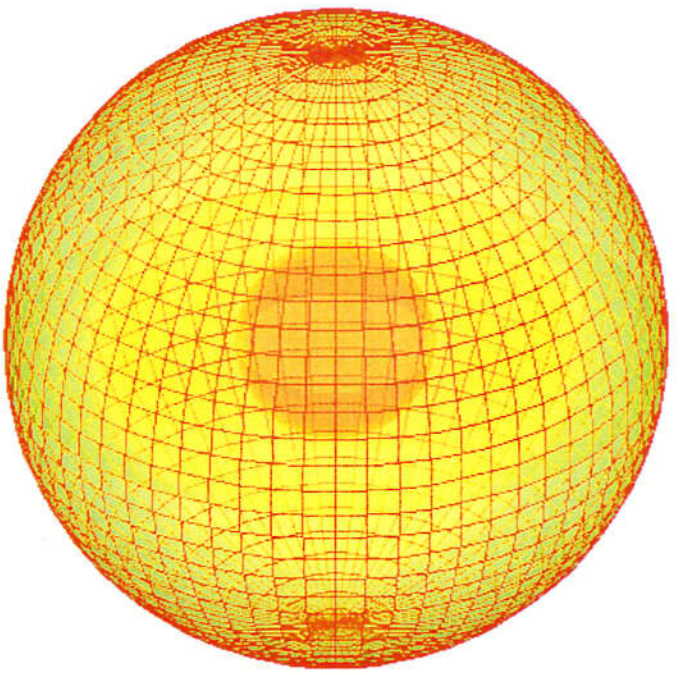

Figure 2.1: Sketch of the simulation geometry of Kageyama-Sato MHD dynamo model.

2.2 Basic Equation

2.2.1 Normalization

It is convenient to deal with the MHD dynamo equations in non-dimensional form. So the following normalizations are used:

1. Length unit: the radius r_o of the outer boundary;
2. Density unit: the density ρ_o at the outer boundary;
3. Temperature unit: the temperature T_o at the outer boundary;
4. Velocity unit: $\sqrt{R_* T_o}$;

5. Time unit: $r_o/\sqrt{R_* T_o}$;

6. Magnetic induction unit: $\sqrt{\mu_0 \rho_o R_* T_o}$.

Here R_* is a gas constant[63] and μ_0 is the permeability of free space.

2.2.2 MHD Equation

The governing equations in MHD dynamo problem are the equations of fluid motion, pre-Maxwell equations, i.e., the Maxwell equations with the displacement current neglected, and the heat equation.

In Kageyama-Sato model, an ideal gas approximation is used for the fluid, and the Navier-Stokes equations for the equations of fluid motion. The self-gravity of the fluid and the centrifugal force are ignored[64]. So the full set of non-dimensional MHD equations with gravity included in a reference frame rotating with the sphere shell include the following equations.

The equations of fluid motion:

$$\frac{\partial \rho}{\partial t} = -\nabla \cdot (\rho \mathbf{v}) \tag{2.1}$$

$$\rho \frac{d\mathbf{v}}{dt} = -\nabla p + \mathbf{J} \times \mathbf{B} + \rho \mathbf{g} + 2\rho \mathbf{v} \times \mathbf{\Omega} + \mu \left[\nabla^2 \mathbf{v} + \frac{1}{3} \nabla (\nabla \cdot \mathbf{v}) \right] \tag{2.2}$$

$$\mathbf{g} = -\frac{g_0}{r^2} \hat{\mathbf{r}} \tag{2.3}$$

The generalized heat equation:

$$\frac{1}{\gamma - 1} \frac{dp}{dt} = -\frac{\gamma}{\gamma - 1} p \nabla \cdot \mathbf{v} + \kappa \nabla^2 T + \eta \mathbf{J}^2 + \Phi \tag{2.4}$$

$$\Phi = 2\mu \left[e_{ij} e_{ij} - \frac{1}{3} (\nabla \cdot \mathbf{v})^2 \right] \tag{2.5}$$

$$e_{ij} = \frac{1}{2} \left(\frac{\partial v_i}{\partial x_j} + \frac{\partial v_j}{\partial x_i} \right) \tag{2.6}$$

The equation of state for the fluid using ideal gas approximation:

$$p = \rho T \tag{2.7}$$

The magnetic field equations:

$$\mathbf{B} = \nabla \times \mathbf{A} \tag{2.8}$$

$$\mathbf{J} = \nabla \times \mathbf{B} \tag{2.9}$$

$$\frac{\partial \mathbf{A}}{\partial t} = -\mathbf{E} \tag{2.10}$$

The generalized Ohm's law:

$$\mathbf{J} = \frac{1}{\eta}(\mathbf{E} + \mathbf{v} \times \mathbf{B}) \tag{2.11}$$

Here ρ, p, T, $\mathbf{v}$, $\mathbf{B}$, $\mathbf{A}$, $\mathbf{J}$, and $\mathbf{E}$ are density, pressure, temperature, velocity, magnetic induction, vector potential, current density, and electric field, respectively. (Note: from this Chapter on, the magnetic induction $\mathbf{B}$ will be referred to as the magnetic field.) The ratio of the specific heats $\gamma(= 5/3)$, viscosity μ, thermal diffusivity κ, and electrical resistivity η are assumed to be uniform constants. $\mathbf{g}$ is the gravity acceleration, $\hat{\mathbf{r}}$ is the radial unit vector, and g_0 is a constant.

2.3 Numerical Method and Techniques

2.3.1 Coordinate System and Numerical Method

The MHD equations in Section 2.2.2 are numerically solved in spherical coordinates (r, θ, ϕ), where r is radius $(r_i < r < r_o)$, θ is colatitude $(0 \leq \theta \leq \pi)$, and ϕ is longitude $(0 \leq \phi \leq 2\pi)$. The polar axis $\theta = 0$ is the direction of rotation. The plane $\theta = \pi/2$ is called the equatorial plane. The plane $\phi =$ constant is called the Meridian cross section.

The full set of MHD equations are solved by the finite difference method[66]. The second-order finite difference method is used for spatial derivative and the fourth-order Runge-Kutta-Gill method for time integration.

Uniform grid points are used for three coordinate directions, respectively. The grid numbers are 50 for radial direction, 38 for latitudinal direction, and 64 for longitudinal direction.

2.3.2 Numerical Techniques

There are two numerical difficulties in solving the MHD equations in spherical coordinates by using the finite-difference method. One is the severity of Courant-Friedrichs-Lewy conditions on the time step due to the concentrated grid points near the pole. Another is the pole singularity problem. The first one is successfully overcome by smoothing the variables near the pole [64]. The vector potential **A** is used in the electromagnetic induction equation because smoothing should not applied to **B** as it produces a small magnetic monopole component. The second difficult is removed by using the limitation forms of MHD equations on the pole. Thus the MHD equations on the pole can be transformed into a nonsingular form. We place grid points on the pole and solve the transformed MHD equations on these grids by the finite-difference method [41].

2.4 Boundary and Initial Conditions

2.4.1 Boundary Condition

The boundary conditions for the temperature are: the inner boundary temperature T_i and outer boundary temperature T_o are kept uniform and constant ($T_i > T_o$) during the whole simulation, respectively.

The no-slip boundary conditions are used for fluid velocity field at the inner and outer boundaries.

$$\mathbf{V} = 0 \text{ at } r = r_i, 1 \tag{2.12}$$

For the magnetic field, we adopt the radial field assumption [30] in which the magnetic field has only the radial component at the inner and outer boundaries.

$$E_r = \frac{\partial}{\partial r}(rE_\theta) = \frac{\partial}{\partial r}(rE_\phi) = 0 \text{ at } r = r_i, 1 \tag{2.13}$$

2.4.2 Initial Condition

The simulation starts from an unstable hydrostatic equilibrium state as follows in absence of external magnetic field,

$$T(r) \;=\; 1 - \beta + \frac{\beta}{r} \tag{2.14}$$

$$\rho(r) = [T(r)]^m \tag{2.15}$$

$$m = \frac{g_0}{\beta} - 1 \tag{2.16}$$

A thermal convection instability grows as a weak random noise is superimposed upon the initial temperature profile. When the convection motion reaches a steady thermal convection state, it takes the form of convection columns regularly spaced round the axis of rotation and drifting in longitude about that axis[64]. Then a random seed magnetic field is added to the system, and the magnetic field can develop through the dynamo action.

2.5 Dimensionless Numbers

The Dimensionless parameters are Prandtl number P_r, magnetic Prandtl number P_m, Taylor number T_a, modified Rayleigh number R_a, and Roberts number R_R defined by

$$P_r = \frac{\mu}{(\gamma - 1)\kappa} \tag{2.17}$$

$$P_m = \frac{\mu}{\eta} \tag{2.18}$$

$$T_a = \left[\frac{2\Omega(r_o - r_i)^2}{\mu}\right]^2 \tag{2.19}$$

$$R_a = \frac{g_0 \left\{\left[\frac{\gamma}{\gamma-1}\right]\beta - g_0\right\}(r_o - r_i)^4}{\mu\kappa} \tag{2.20}$$

$$R_R = \frac{\kappa}{\eta} \tag{2.21}$$

Note that the Rayleigh number of a stratified fluid is a function of the depth[67]. Here we measure the local Rayleigh number on the outer boundary.

Chapter 3

Simulation Results

3.1 Simulation Parameters

Due to huge computation cost in MHD dynamo numerical simulation, it is impossible to make a comprehensive parameter study. In our simulations, we change three physical parameters, namely, the electrical resistivity, the angular velocity of rotation, and the inner temperature. The other parameters are kept unchanged.

The basic equation of MHD dynamo problem is the magnetic induction equation, as shown in equation (1.8). Generally, the magnetic Reynolds number, which depends on the electrical resistivity of electrically conducting fluid, should be larger enough to maintain the dynamo action. For self-excitation of a magnetic field it has to be at least greater than 1. For typical dynamos as the Earth outer core, it supposed to be of the order of 100. So we choose the electrical resistivity as our first parameter.

For the convection-driven dynamo in a rotating spherical shell, the strength of the thermal driving is measured by the Rayleigh number, which depends on the temperature difference of inner and outer boundaries. In Kageyama-Sato model, the temperature on the outer boundary is fixed and kept to be uniform. Thus the inner boundary temperature is an important parameter for the convection motion, and is chosen as the second parameter.

Rotation is a fundamental condition for MHD dynamo. The Coriolis force, which makes the rotating MHD quite different from the classical MHD, takes a central role of in the dynamics of the rotating shell. Many works have done on it[29, 68, 71]. The expression of the Coriolis force is $2\rho\mathbf{V} \times \mathbf{\Omega}$. So the angular velocity $\mathbf{\Omega}$ of spherical shell rotation is

one of important parameters in the MHD dynamo problem.

In our simulations, we keep the following parameters $r_i = 0.3$, $g_0 = 1.0$, $\kappa = 4.243 \times 10^{-3}$ and $P_r = 1.0$ unchanged, and change only Ω, T_i and η. We carry out the simulations for two different rotation velocities, $\Omega = 7.0$ and 9.0. To investigate the possible effects of the electrical resistivity on magnetic field generation and reversal, we compare five dynamo simulations, in which the inner boundary temperature $T_i = 3.5$ and rotation velocity $\Omega = 7.0$ are fixed, with different electrical resistivities $\eta = 4.0 \times 10^{-4}$, 3.0×10^{-4}, 2.7×10^{-4}, 2.5×10^{-4}, and 1.0×10^{-4}. At rotation velocities $\Omega = 9.0$, three dynamo simulations with different temperatures of inner boundary, $T_i = 3.5$, 5.0, and 8.0, are carried out.

The detail physical parameters used in our simulations are listed in Table 3.1. It should be noted that Case (3) is the simulation result of Reference [44].

Table 3.1: Simulation parameter set and corresponding reversal status. Ω is angular velocity of rotation; T_i temperature of inner boundary; η electrical resistivity; T_a Taylor number; R_a local Rayleigh number on the outer boundary, and P_m magnetic Prandtl number.

Case No.	(1)	(2)	(3)*	(4)	(5)	(6)	(7)	(8)	(9)
Ω	7.0	7.0	7.0	7.0	7.0	7.0	9.0	9.0	9.0
T_i	3.5	3.5	3.5	3.5	3.5	3.5	3.5	5.0	8.0
$\eta(\times 10^{-4})$	4.0	3.0	2.8	2.7	2.5	1.0	1.0	1.0	1.0
$T_a(\times 10^6)$	5.88	5.88	5.88	5.88	5.88	5.88	9.72	9.72	9.72
$R_a(\times 10^4)$	3.36	3.36	3.36	3.36	3.36	3.36	3.36	6.57	13.0
P_m	7.07	9.43	10.1	10.5	11.3	28.3	28.3	28.3	28.3
Reversal†	N	N	T	R	R	R	R	R	R

† N: no reversal, T: transient, R: repeated. * The result of Reference [44].

The simulation results will be briefly discussed in the next section.

3.2 Overview of the Simulation Results

Our dynamo simulation starts from the steady thermal convection motion state which takes the form of convection columns regularly spaced round the axis of rotation and

drifting in longitude about that axis by adding a very weak random seed magnetic field to the spherical shell region. The magnetic field can develop through the dynamo action according to the magnetic induction equation (1.8).

The magnetic field reversal statuses of our MHD dynamo numerical simulation results are summarized in Table 3.1.

Among the nine cases, the case (4) in Table 3.1 is our standard simulation run, in which the thermal diffusion time is 115, the magnetic diffusion time is 1815. This standard simulation run is continued for a very long simulation time. In whole simulation evolution, the magnetic field reverses its polarity irregularly many times. Reversal appears to occur without any regular rule. It does reverse suddenly and the reversal does continue endlessly. As a whole, it is unlikely that the existence of one polarity predominates over the other. Based on its time evolution behaviors, we have presented the conditions of the magnetic field reversal. By analyzing the relationship of the structure of the convection motion and the structure of the magnetic field, we have presented a mechanism of magnetic field reversal. The detail simulation results of case (4) will be given in Chapters 4, 5, and 6.

The effects of electrical resistivity and the temperature difference between the inner and outer boundary to the generation and reversals of the magnetic field are also among our research concerns.

Parameter runs find that dynamo action is strongly dependent on electrical resistivity. When the electrical resistivity is high, the generated magnetic field possesses weak energy, and the convection motion of the fluid is not greatly modified. Therefore, the magnetic field generated by the convection motion maintains its polarity very well. Cases (1) and (2) show no magnetic field reversal, the dynamo systems develop to steady states in which total kinetic and magnetic energies keep almost constant and dipole fields do not reverse their polarities. As the electrical resistivity decreases, the generated magnetic energy increases, the time evolutions of total convection kinetic energy and generated magnetic energy make flip-flop alternations between high energy states and low energy states. The magnetic field reversals are observed. A transient reversal occurs in Case (3), which is the previous simulation (see Reference [44]), and the dynamo system finally reaches to a steady state. In Cases (4) and (5), the magnetic field reversals occur only in high energy states. The reversal does continue endlessly in Case (4). For Case (6) of the smallest electrical resistivity, the generated magnetic field becomes considerably strong. There is only high energy state in the energy evolution. The dipole reversals occur at a high energy state too.

The effects of inner boundary temperature to the generated magnetic field are studied

in Cases (7), (8), and (9). As the temperature at inner boundary increases, the thermal convection becomes strong, so the kinetic energy increases. Fast rotation acts to inhibit convection. For the dynamo action, the increase of rotation velocity leads to the decreases of both the total convection energy and the total magnetic energy and big fluctuation in total magnetic energy. The magnetic field changes from dipolar dominant type to non-dipolar dominant type.

The results are presented in Chapter 7.

Chapter 4

Repeated and Sudden Reversals of Magnetic Field

In this chapter, we shall discuss a long time simulation result of our standard run, or Case (4) in the Table 3.1, in which the magnetic field reverses its polarity repeatedly and suddenly and the total kinetic and magnetic energies exhibit a flip-flop alternation between a high energy state and a low energy state[69]. Based on this standard run, the conditions of the magnetic field reversal will be given.

4.1 Initial Convection Motion

The numerical simulation starts from an unstable hydrostatic equilibrium state described in Section 2.4.2 by introducing a weak random temperature noise.

The fluid motions are driven by thermal convection. When the convection motion reaches a steady thermal convection state, it takes the form of convection columns regularly spaced round the axis of rotation and drifting in longitude about that axis[25, 26, 27, 29, 64, 65, 70, 71, 72, 73]. There are two kinds of convection columns, the cyclonic column and the anticyclonic column. The cyclonic (anticyclonic) column rotates in the same (opposite) direction as the spherical shell rotation. The flow in a cyclonic (anticyclonic) column is directed toward (away from) the equatorial plane[64]. In the case (4), the initial convection column pattern is shown in Figure 4.1. The structure of convection columns is visualized by the isosurface of the axial component of the vorticity (|axial vorticity| = 1, yellow for +1, blue for -1), a component of the vorticity along the direction of the

rotation axis. The velocity distribution and density contour in the equatorial plane keep almost unchanged westward-drifting patterns at constant angular velocity with 5 pairs of the convection columns as shown in Figure 4.2. It is clear from the velocity distribution in the meridian plane that the convection motion pattern shows a good north-south symmetry around the equatorial plane.

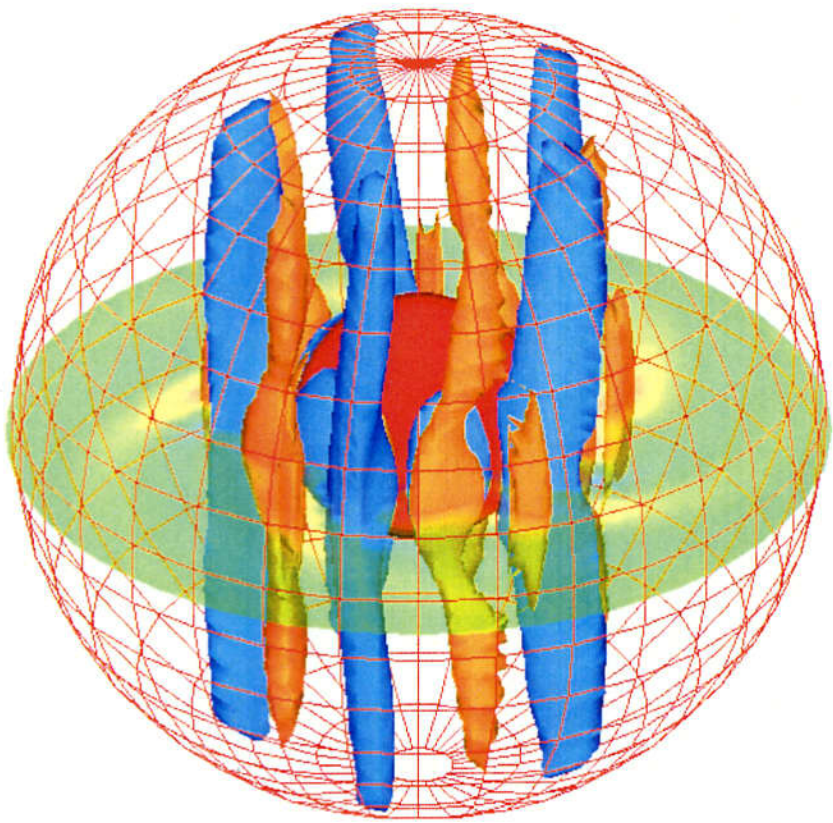

Figure 4.1: The convection columns expressed by the isosurface of the axial component of the vorticity (|axial vorticity| = 1, the yellow one for +1 is called the cyclonic column; the blue one for -1 is called the anticyclonic column.) when the convection motion reaches steady state.

Our dynamo simulation starts from the steady thermal convection motion state shown in Figure 4.1 and Figure 4.2 by adding a very weak random seed magnetic field to the spherical shell region. The magnetic field can develop through the dynamo action according to the magnetic induction equation (1.8).

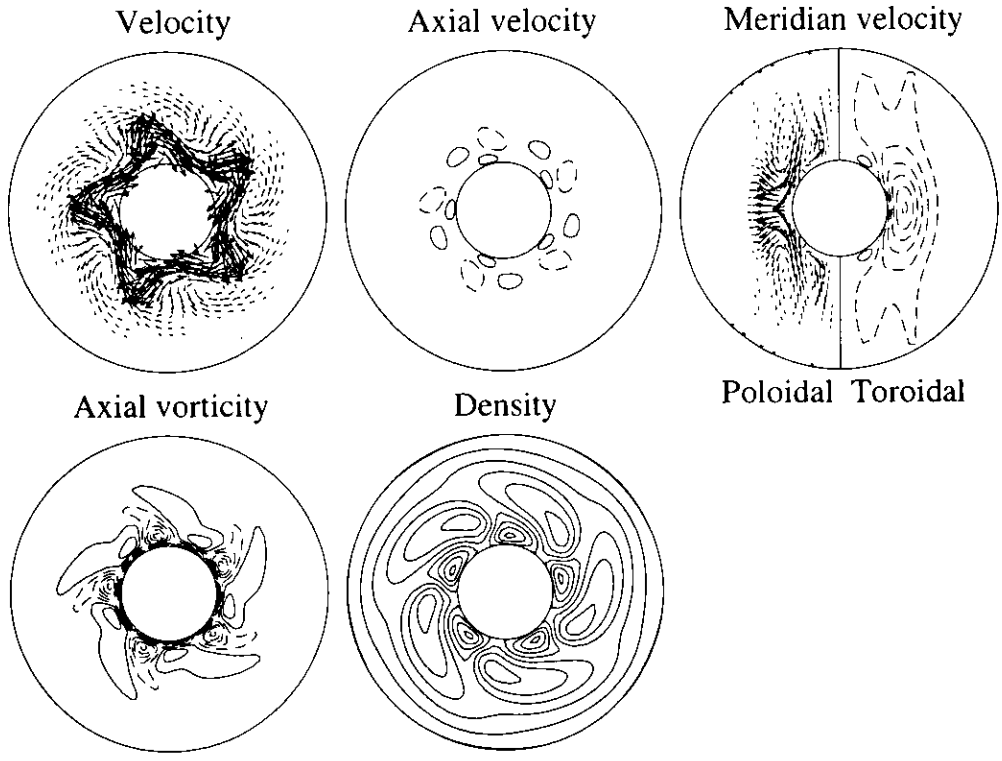

Figure 4.2: Steady pattern of convection motion. Top: the velocity distributions of fluid in the equatorial plane (left: velocity vector; middle: axial component contour) and meridian plane (right: left half for poloidal component, and right half for toroidal component contour). Bottom: the axial component contour of vorticity (left) and density contour (middle) in the equatorial plane.

4.2 Long Time Evolution

Our dynamo model, or Kageyama-Sato model, is a convection-driven MHD dynamo model. The inner spherical boundary is kept to be a constant high temperature and the outer boundary to be a constant low temperature. The heat flux transfers from the inner boundary to the outer boundary. Kinetic energy of fluid and magnetic energy can be used to evaluate the convection motion and generated magnetic field. The total kinetic

and magnetic energy are defined, respectively, by

$$E_K = \int\int\int \frac{1}{2}\rho \mathbf{V}^2 dV \tag{4.1}$$

$$E_M = \int\int\int \frac{1}{2}\mathbf{B}^2 dV \tag{4.2}$$

Here $\mathbf{V}$ is the velocity of fluid and $\mathbf{B}$ is the magnetic field. The integrals are carried out in the whole region of the spherical fluid shell ($r_i \leq r \leq r_o$; $0 \leq \theta \leq \pi$; $0 \leq \phi \leq 2\pi$).

Usually, the magnetic field polarity is described by the direction of magnetic dipole moment at the original point of the spherical coordinate, which is defined by

$$\mathbf{m} = \int\int\int \frac{1}{2}\mathbf{r} \times \mathbf{J}(\mathbf{r}) dV \tag{4.3}$$

Here $\mathbf{r}$ is a position vector and $\mathbf{J}(\mathbf{r})$ is the electrical current density. The integral region is the whole region of the spherical fluid shell.

The dipole polarity is expressed by pole latitude (latitude differs from colatitude by $\frac{1}{2}\pi$), an angle between magnetic dipole moment vector $\mathbf{m}$ and the equatorial plane. The precession of the magnetic dipole moment is expressed by its longitude angle ϕ.

The long-run-simulation of the dipole field reversal of our standard run is shown in Figure 4.3. The top panel shows the polarity changes of the generated dipole field (red). Evidently, the dipole field reverses its polarity irregularly and swiftly. Reversal appears to occur without any regular rule. It does reverse suddenly and the reversal does continue endlessly. As a whole, it is unlikely that the existence of one polarity predominates over the other. The equivalence between normal and reversal polarity states can be understood in the following way. Under a transformation of $\mathbf{B} \rightarrow -\mathbf{B}$, the Lorentz force term [$\mathbf{J} \times \mathbf{B} = (\nabla \times \mathbf{B}) \times \mathbf{B}$] and Joule heat term [$\mathbf{J}^2 = (\nabla \times \mathbf{B}) \cdot (\nabla \times \mathbf{B})$] keep the same values. Therefore, the MHD equations in Section 2.2.2 keep unchanged. In other words, if a fluid motion can support a magnetic field $\mathbf{B}$, then this fluid motion also can support another magnetic field $-\mathbf{B}$. Certainly, these two magnetic fields possess different polarities.

The second panel of Figure 4.3 shows the evolutions of the total magnetic energy (red) and the total convection (kinetic) energy (black). In the whole evolution, the total magnetic energy is higher than the total convection energy. It appears that both of magnetic and convection energies have two kind of energy states: high energy state and low energy state. The total magnetic energy in low energy states is nearly the same level as the total convection kinetic energy in high energy states. Interestingly, the total

magnetic and kinetic energies exhibit a flip-flop alternation between a high energy state and a low energy state[44]. On close examination of the first panel and second panel, one can clearly recognize a very important and significant fact that reversal occurs only at a high energy state.

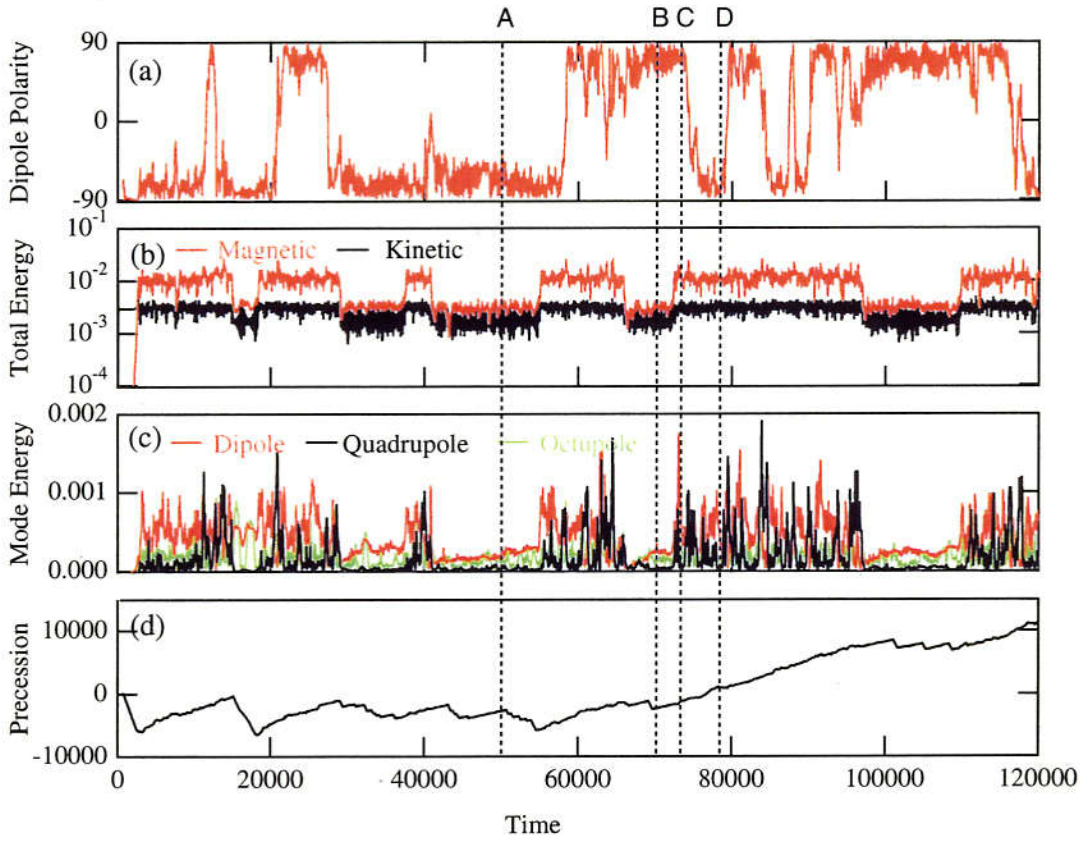

Figure 4.3: Time evolutions of (a) the polarity of dipole field (pole latitude in degree), (b) the total kinetic energy (black) and magnetic energy (red), (c) the mean magnetic energy densities of the dipole (red), the quadrupole (black) and octupole (green) modes at the outer boundary, and (d) precession of magnetic dipole moment (in degree).

The mean magnetic energy density on the outer boundary of the shell can be expressed as the sum of contributions from each spherical harmonic. The generated magnetic field $B_r(1, \theta, \phi)$ and the mean magnetic energy density at the outer spherical boundary are

written in terms of spherical harmonics as following

$$B_r(1,\theta,\phi) = \sum_{l=1}^{\infty}\sum_{m=-l}^{l} a_{lm}Y_{lm}(\theta,\phi) \tag{4.4}$$

$$\int_0^{\pi}\int_0^{2\pi} B_r^2 \sin\theta d\theta d\phi = \sum_{l=1}^{\infty}\sum_{m=-l}^{l} |a_{lm}|^2 \tag{4.5}$$

$$E(l) = \sum_{m=-l}^{l} |a_{lm}|^2 \tag{4.6}$$

Here the $Y_{lm}(\theta,\phi)$ are surface harmonics of degree l and order m[74], and $E(l)$ is the mean magnetic energy density of the contribution from spherical harmonic of degree l.

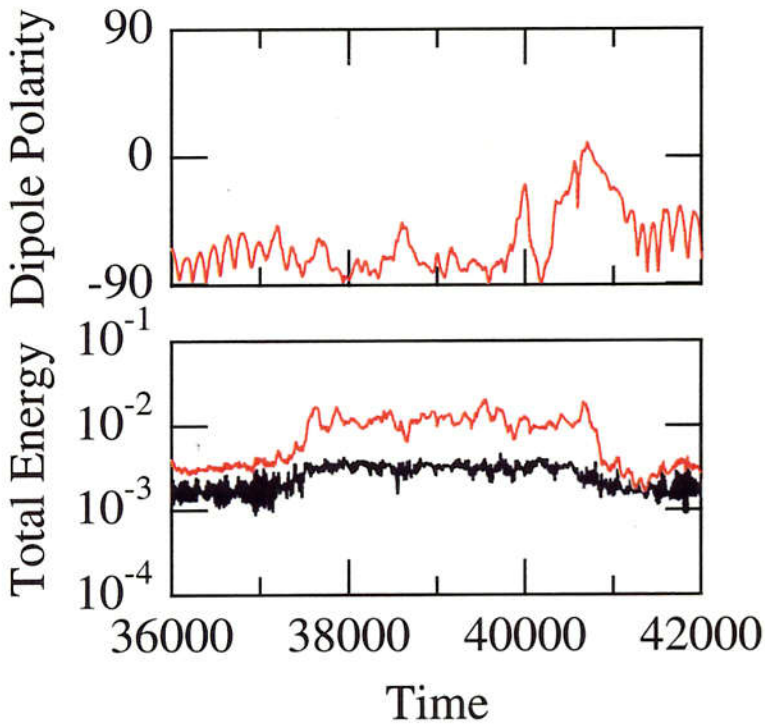

Figure 4.4: An interrupted reversal of magnetic field. Top panel shows time evolution of the polarity of dipole field. Bottom panel shows time evolution of the total kinetic energy (black) and magnetic energy (red).

The third panel of Figure 4.3 shows the time evolutions of the three dominant magnetic

harmonic modes at the outer boundary (dipole – red, quadrupole – black, octupole – green). In most of the whole simulation time, the dipole mode is the strongest, which means that the generated magnetic field is dipole-dominated. In comparison with the first panel of Figure 4.3, we find that the variations of the harmonic modes in the strength in low energy states are weaker than those in high energy states.

It is interesting and suggestive to observe a tendency that the quadruple mode tends to become excited and grow comparable or larger than the dipole component as the dipole polarity is reversed. It should be noted that in high energy states, when the mean energy density of quadrupole component is stronger than that of dipole, the dipolar field display some tendency to reverse. Sometime the dipole field achieves a success reversal. The detail will be discussed in Section 4.4.

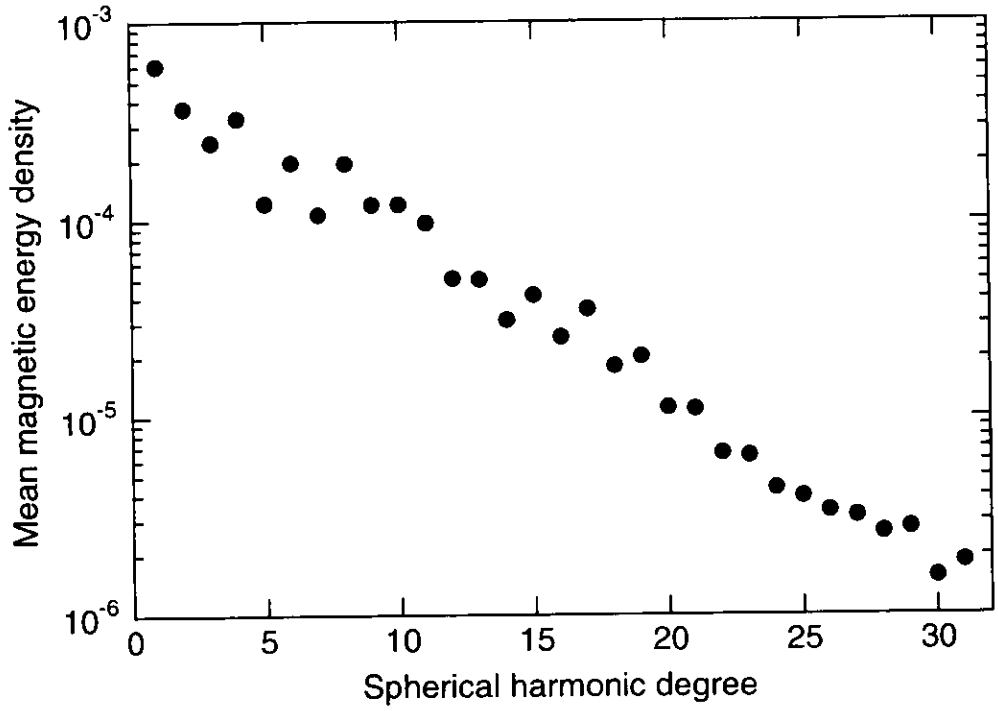

Figure 4.5: A snapshot of the mean magnetic energy density at the outer boundary as a function of spherical harmonic degree.

The bottom panel of Figure 4.3 shows the precession of the tip of the dipole moment around the rotation axis. One can see that the precession is basically eastward in the high energy state and westward in the low energy state, but that there seems to be no

meaningful correlation with dipole reversal.

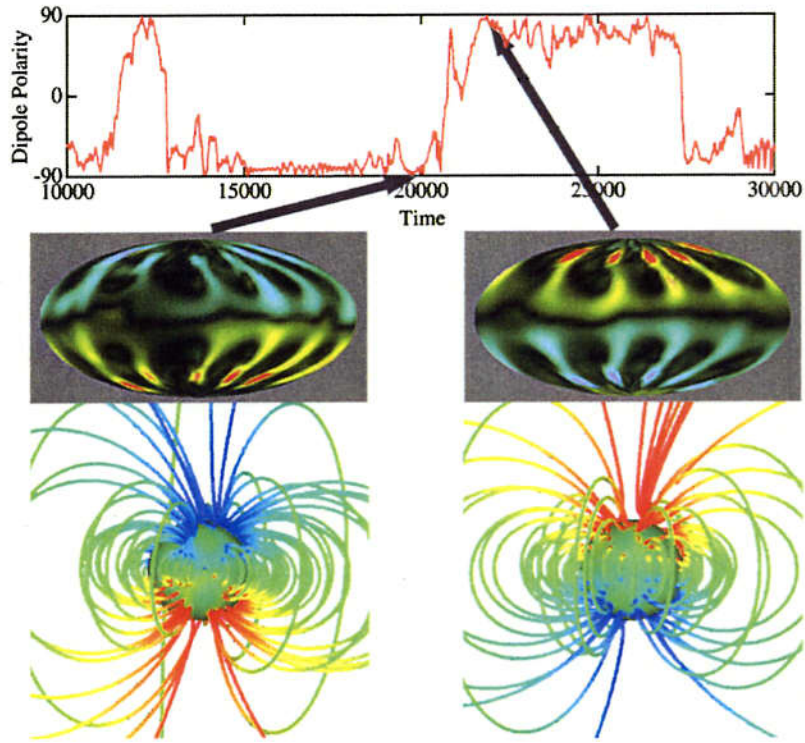

Figure 4.6: Two snapshots of the generated magnetic fields before and after reversal. The top panel indicates the magnified time evolution of the dipole polarity in the range of time = 10000 – 30000. The middle panels show the color-coded representation of the radial component at the outer boundary of the dynamo shell (red directed outward and blue inward). The bottom panels show the magnetic field lines extending out of the shell before (time = 19854) and after (time = 21850) the reversal around time = 21000 where the direction of a magnetic field line is color-coded by red to blue.

Furthermore, it appears that reversal occurs when a high energy state continues for a certain duration. This tendency is endorsed when one sees no reversal in the high energy state that lasted relatively short around time = 40000 (see Figure 4.4). In this state one can certainly notice an indication of reversal, but it ceases on the way. This ceasing was obviously interrupted on the way by the transition from the high energy state to the low energy state. In this respect, it should be noted that the previous statement given in the previous paper [44] that the reversal was accompanied by the energy transition is

misleading. In fact, the long run of that case (i.e., case (3) in Table 3.1) finds that the reversal is only transient and the system finally reaches to a steady state.

In most time of our simulation evolution, the mean energy density in the dipole field at the outer boundary exceeds that in any other harmonic. Generally, the energy in high spherical harmonic degree becomes weak with the increase of spherical harmonic degree. Figure 4.5 shows a snapshot of the mean magnetic energy density at the outer boundary as a function of spherical harmonic degree.

Shown in Figure 4.6 are the magnetic field configurations just before and after one of the dipole reversals. The top panel shows the dipole polarity change in the range of time = 10000 - 30000 on which the sampling times are indicated by arrows. The middle panels are the corresponding color-coded contour maps of the radial component of the magnetic field at the outer boundary of the dynamo shell and the bottom ones are the magnetic field lines out of the shell before and after the reversal. It is clearly shown that the magnetic fields before and after the reversal are dipole-dominated and similar in the structures except different magnetic polarities.

4.3 Bi-Stable System for Magnetic Polarity

The energy state, both magnetic and kinetic, of an MHD dynamo in a rotating spherical shell is a bi-stable system. The dynamo system can take a high energy state and a low energy (as shown in Figure 4.3). More specifically, the system flip-flops in an irregular fashion between a high energy state and a low energy state. The different energy states correspond to different magnetic field configurations and convection patterns. A reversal occurs only in a high energy state (as shown in Figure 4.3) and only if the high energy state keeps over a certain period (as shown in Figure 4.4).

What makes two kinds of energy states different? Now, we make a comparison between the convection motions in different energy states. The convection columns drift in longitude about the axis of rotation. During the whole simulation both the number of convection columns and their drift directions are not fixed. There are mainly two kinds of states: fast drift states and slow drift states. In fast drift states, the convection columns drift westward and keep almost unchanged structures. While in slow drift states, they mainly drift eastward and easily change their structures. Figure 4.7 shows the time evolution of the radial component of the velocity at the middle of the shell in the equatorial plane, which can be used to illustrate the drift behaviors of convection columns. The black region corresponds to the radial component of the velocity outward-directed, and

the white region the radial component of the velocity inward-directed. The red line shows the pole latitude of the dipole moment. In order to clearly see the evolution of convection, here we just show a part of whole simulation from time = 60000 to 80000. The number of convection columns and their drift directions and velocities are clearly recognized in this figure. The occurrence of dipole reversal is always accompanied by the change of thermal convection motion. On the contrary, it is not true that the change of convection motion must lead to a dipole reversal. This point is obviously shown in the figure.

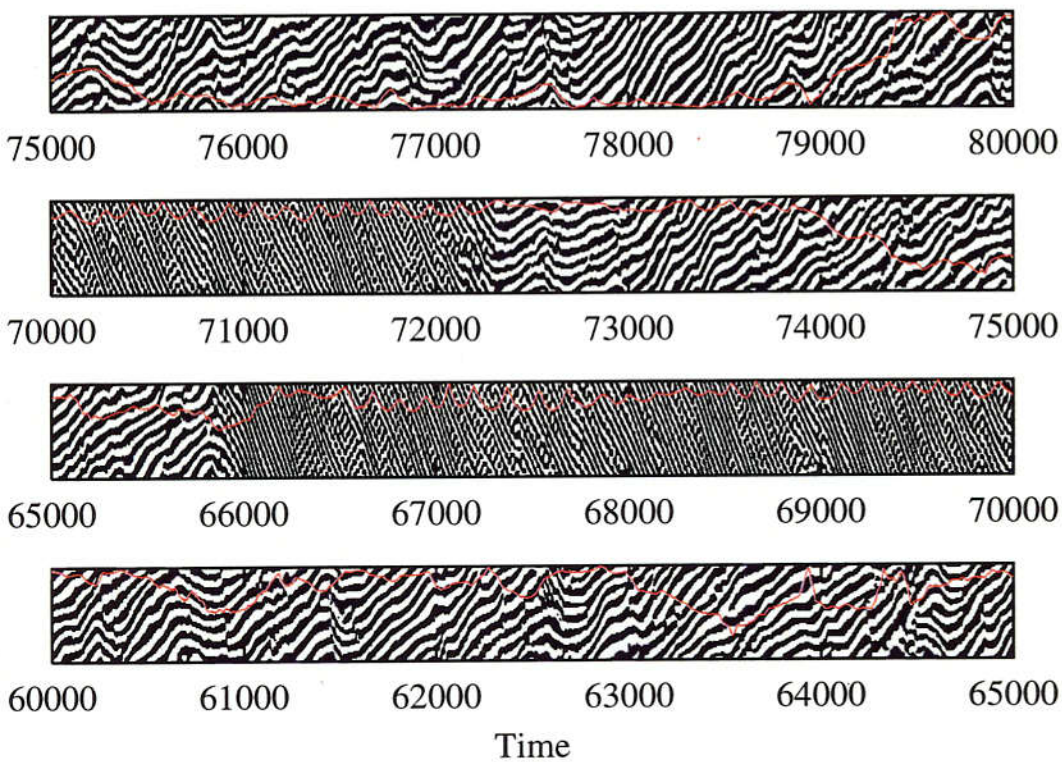

Figure 4.7: The drift motion of the convection columns in the equatorial for time = 60000 – 80000. The horizontal axis is the time, and the vertical axis is the longitude ($0° \leq \phi \leq 360°$). The black (white) region at each time denotes the rising (sinking) fluid, the radial component of velocity, in the equatorial plane at $r = 0.65$. The red line shows the pole latitude function with time.

The comparison between Figure 4.3(a) and Figure 4.7 shows that a slow drift state corresponds to a high energy state and a fast drift state a low energy state. Convection columns drift slowly in a high energy state, and drift fast in a low energy state.

The magnetic dipole field reverses its polarity many times, and at irregular time interval. The process of each reversal lasts very short time. In other words, a magnetic field reversal takes place quickly, as the magnetic field of the Earth [1, 2]. In the most of other time, the magnetic field shows a good polarity, namely, the angle between the direction of dipole moment and the rotation axis is small. The total duration when dipole moment directs to the north is nearly equal to the total duration when it directs to the south. This fact means that the dynamo action in a rotating spherical shell does not prefer to be in one polarity state rather than in another. Figure 4.8 shows the trajectory of the south magnetic pole of the dipole at outer surface of the spherical shell corresponding to Figure 4.7 from time = 60000 to 80000.

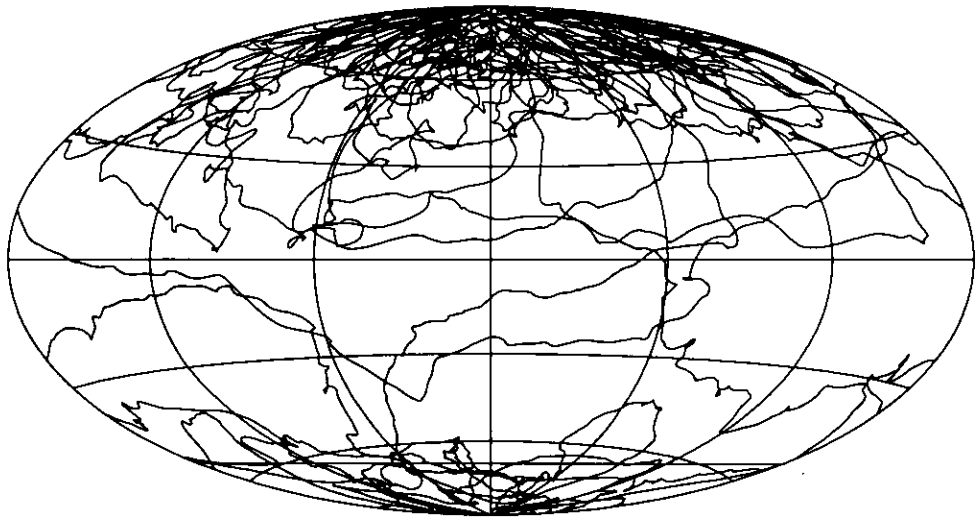

Figure 4.8: The trajectory of the south magnetic pole of the dipole at outer surface of the spherical shell shown in a Hammer-Aitoff Projection for time duration from 60000 to 80000.

4.4 Quadrupole Mode Behavior in Reversals

Now we shall consider the property of the magnetic field reversals from the view of the time evolution. In order to see more deeply the relationship between the dipole reversal and the behavior of the quadrupole mode, we plot its evolution on a finer-scale in Figure 4.9, in which the evolutions of the dipole polarity, dipole mode and quadrupole mode are shown.

The strength of the dipole mode is stronger than that of the quadrupole mode in most time of the whole evolution.

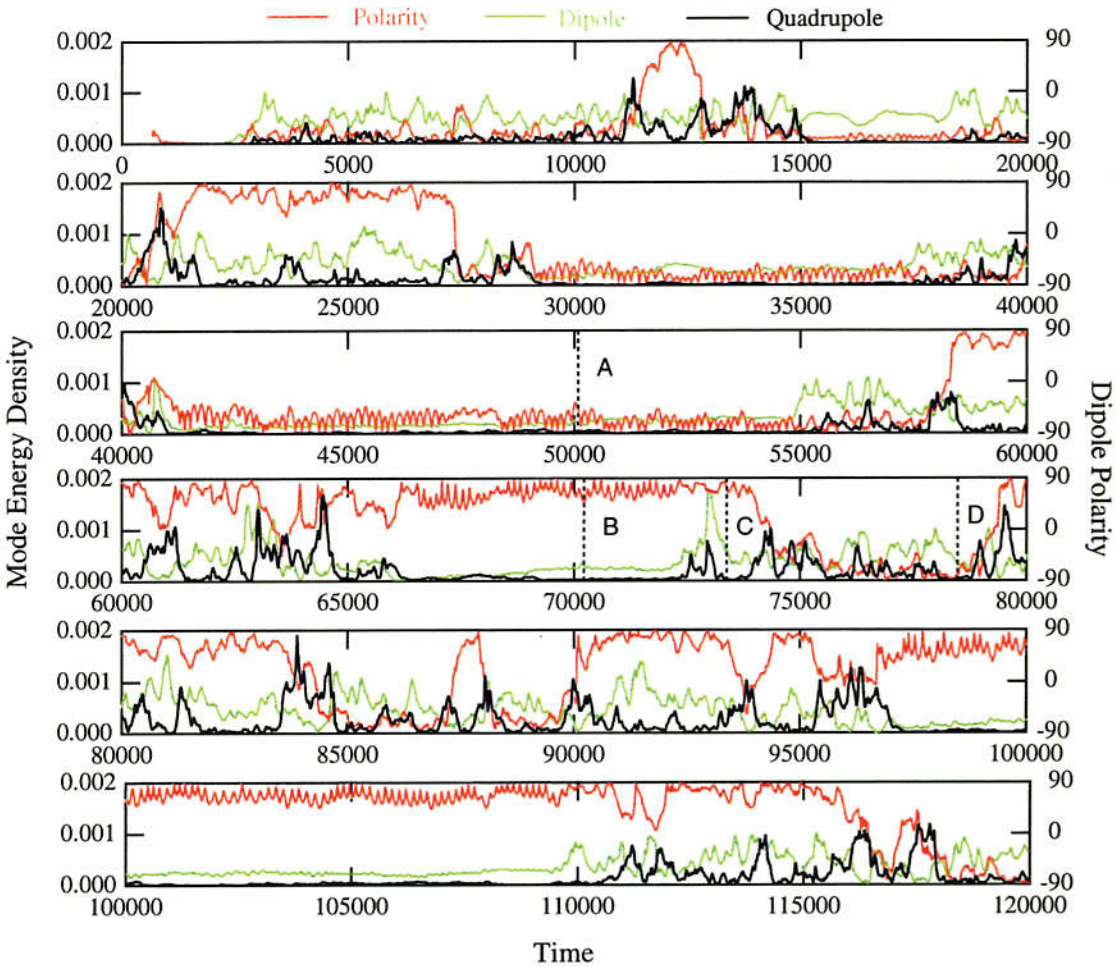

Figure 4.9: Time evolutions of the dipole and quadrupole modes. The red line is for the dipole polarity, the green one for dipole mode, and the black one for quadrupole mode.

Close examination of every magnetic field reversal shown in Figure 4.9 reveals that when a magnetic field reversal takes place the quadrupole mode grows before a magnetic field reversal and becomes stronger and stronger. When a magnetic field reversal occurs, the quadrupole mode is stronger than the dipole mode, and becomes dominant. When a magnetic field completely reverses its polarity, its dipole field grows again and becomes dominant. These facts strongly suggest that the dipole reversal is highly correlated with the growth and dominance of the quadrupole mode.

4.5 Conditions of Magnetic Field Reversal

In the previous Sections, we have discussed the evolutions of kinetic and magnetic energies (Figure 4.3), and dipole and quadrupole modes (Figure 4.9), from which we can obtain the following conditions for magnetic field reversal:

1. The dynamo system is in an high energy state.
2. The high energy state lasts for a certain duration.
3. The quadrupole mode of the magnetic field energy density at the outer boundary is growing prior to the magnetic field reversal.
4. The quadrupole mode exceeds the dipole one on the magnetic field reversal.

The last two conditions are consistent with the suggested correlations between field strengths and reversals[75]. The physical mechanism of magnetic field reversal, which is related to the general structures of the convection motion and the magnetic field, will be discussed in detail in Chapter 5.

Chapter 5

Physical Mechanism of Magnetic Field Reversal

In MHD dynamo, the magnetic field is generated by the convection motion of electrically conducting fluid. The structure and evolution of the magnetic field is determined by how and where it is twisted and sheared by the fluid flow, which itself is influenced by nonlinear magnetic (Lorentz) force.

The main purpose of this Chapter is to understand the physical mechanism of the magnetic field reversal. Because of the strong interaction of the fluid flow and the magnetic field, the dynamics of the convection motion of the fluid is very important in clarifying the reversal mechanism. In this Chapter, we shall give a magnetic field reversal mechanism through analyzing the changes in the structure of the convection motion and the structure of the magnetic field in our standard run[69].

5.1 Structure of Convection Motion

In the exponentially growing phase of magnetic field, the Lorentz force is not strong enough to greatly change the structure of convection motion. The convection motion shows a symmetric feature about the equatorial plane. The generation mechanism of magnetic field is shown clearly in the previous works of Kageyama et al.[42, 43]. The poloidal magnetic field is generated when toroidal field force lines are stretched and deformed by inward flows between cyclonic and anticyclonic convection columns. The toroidal field is generated from the poloidal field by the drifting mean flow in the equator. Because of the

symmetry of the convection motion about the equatorial plane, the structure of the mean magnetic field also shows some symmetry about the equatorial plane. This symmetry makes it difficult for magnetic field to reverse its polarity.

In order to clarify the mechanism of magnetic field reversal, it is helpful to consider the relation of the detail structures of the convection motion and magnetic field in different energy states. It is well known that for the convection motion driven by thermal convection in a rotating spherical shell, there are two kinds of convection columns, the cyclonic column and the anticyclonic column. In the presence of the magnetic field, the long time evolution simulation of our standard run shows that the thermal convection in the rapidly rotating spherical shell also takes the form of columnar cells which are parallel to the rotation axis. The magnetic field structure inside the spherical shell is very complicated. Generally, the magnetic field lines spiral around the convection columns. The fact that the total convection kinetic and magnetic energies show two energy states suggests that these different energy states correspond to the different convection structures and magnetic field structures.

Figure 5.1 shows the structure of convection columns visualized by the isosurface of the axial component of the vorticity for four different times corresponding to two different energy states and two different magnetic polarities. In the low energy states of Times A and B, the numbers of the convection column are fixed, both are seven pairs. The structures of the convection column show comparative good north-south symmetry around the equatorial plane (A and B in Figure 5.1). In the high energy states of Times C and D, the numbers of the convection column are changing with time. The basic structures of the convection column are time-dependent. It is obvious that the north-south symmetry is broken. (C and D in Figure 5.1).

In order to find a further confirmation that the north-south symmetry is broken in high energy states, we need to examine the distributions of the fluid velocity in the equatorial plane and the meridian plane. The axial components of fluid velocities in the equatorial plane shown in the top row of Figure 5.2 verify the break of the north-south symmetry of the convection motion in high energy states. In low energy states of Times A and B, the axial components of fluid velocities in the equatorial plane are very weak. The convection motion is symmetric around the equatorial plane. While in high energy states, the axial components of fluid velocities in the equatorial plane of Times C and D are very strong. The north-south symmetry around the equatorial plane is broken. The existence of the trans-equatorial flows in high energy states suggest that there is a strong interaction of fluid motion between the northern and southern hemispheres. This strong interaction of fluid flow leads to an instability of convection motion, and further leads to the change in

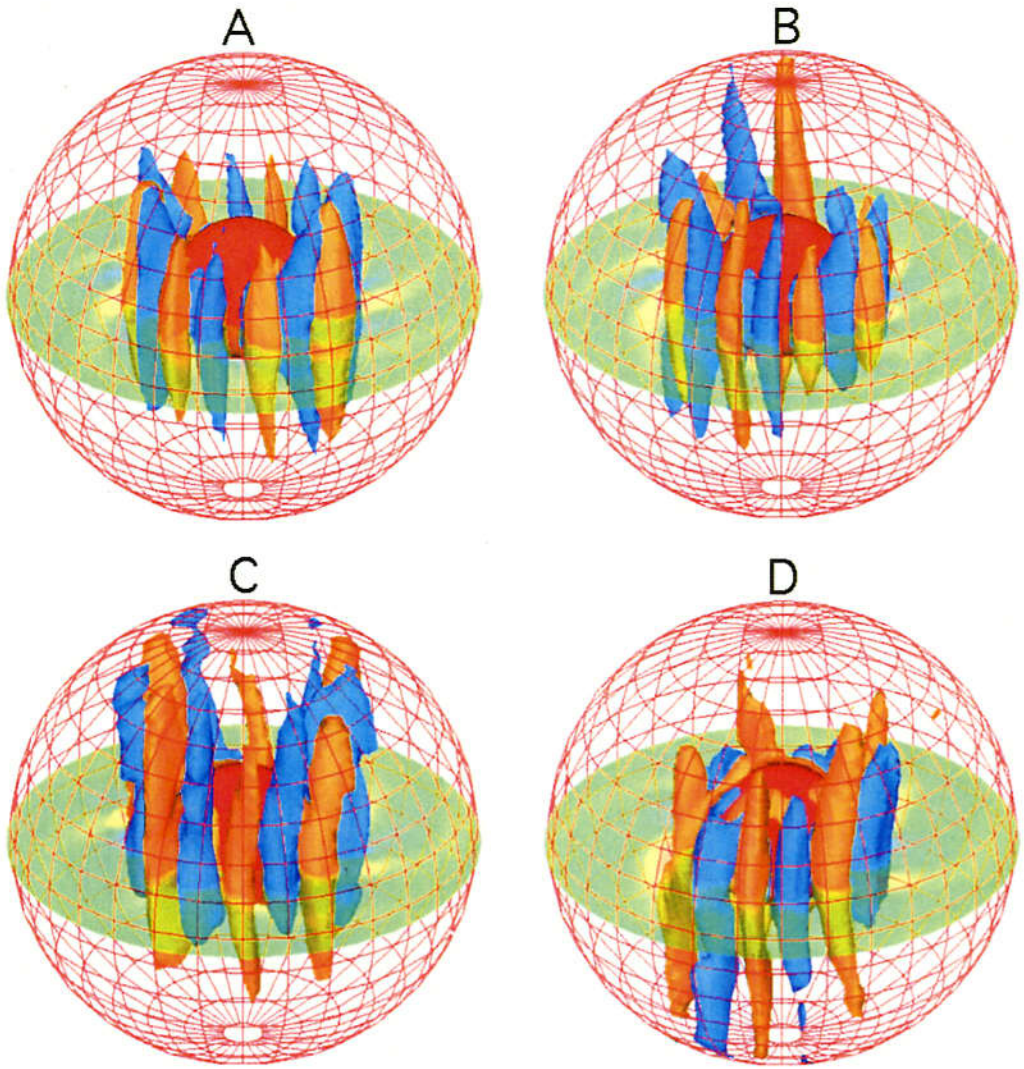

Figure 5.1: The convection columns expressed by isosurface of the axial component of vorticity (red: 1.0, blue: -1.0) in two different energy states. Times A and B are in low energy states, and Times C and D in high energy states (The time positions of A, B, C, and D are marked by dashed lines in Figure 4.3 and Figure 4.9).

the number of convection column.

The distribution of fluid velocity in the meridian plane clearly show the departure from north-south symmetry of convection motion in the high energy states. Now it is interesting to examine the longitudinally averaged fluid velocity. This longitudinally averaged velocity can be decomposed into the poloidal component (A vector in r–θ plane of a spherical coordinate system) and the toroidal component (A vector in ϕ direction). In the low energy states, very good symmetries of the poloidal and toroidal components around the equatorial plane can be seen clearly in the bottom row of Figure 5.2. It is similar to the convection motion in the exponentially growing phase of magnetic field in the previous works of Kageyama et al.[42]. However, in the high energy states, the cases are different. The toroidal components of the velocity show some differences in two hemispheres. The poloidal components of the velocity lose the equatorial symmetry. There exist strong flows across the equatorial plane in Times C and D which are shown clearly in the bottom row of Figure 5.2.

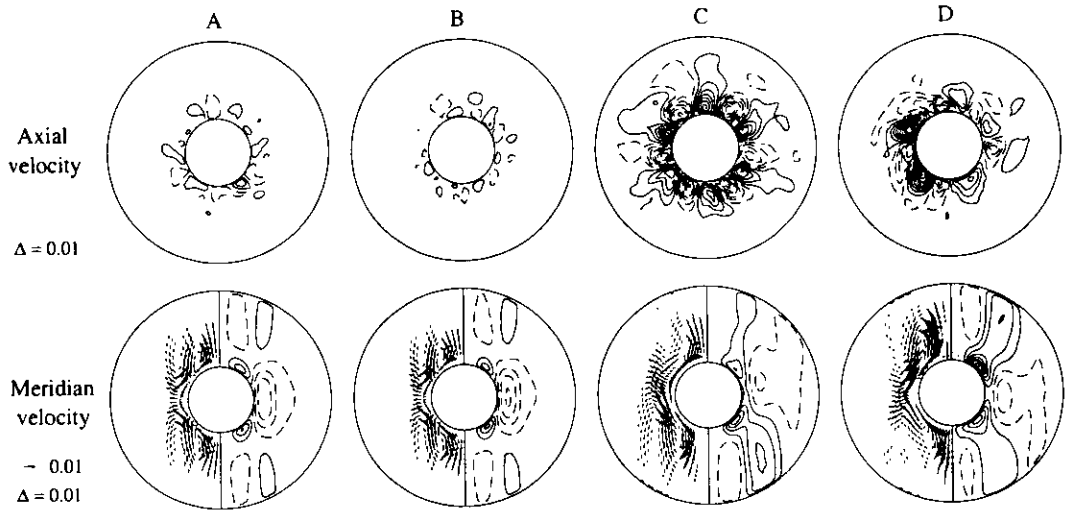

Figure 5.2: The convection motion structures in two different energy states. Times A and B are in low energy states, and Times C and D in high energy states (The time positions of A, B, C, and D are marked by dashed lines in Figure 4.3 and Figure 4.9). Top row: the axial component of the velocity in the equatorial plane. Bottom row: the longitudinally averaged velocity in the meridian plane (left: poloidal vector; right: toroidal component.).

The convection motion in high energy states exhibits the basic columnar structure,

but nevertheless it is time-dependent. The velocity distribution not only in the equatorial plane but also in the meridian plane give us a strong confirmation that the convection motion in the high energy states departs from the north-south symmetry. This departure of north-south symmetry will lead to a magnetic field reversal.

5.2 Structure of Magnetic Field

The magnetic field is generated by the convection motion of the electrically conducting fluid. The magnetic field has a tendency to become parallel or anti-parallel to the convection motion. This tendency can be understood as the magnetic field stretching effect subject to the flow of highly conducting fluid[41]. So the magnetic field pattern is strongly correlated with the fluid flow in the sphere shell.

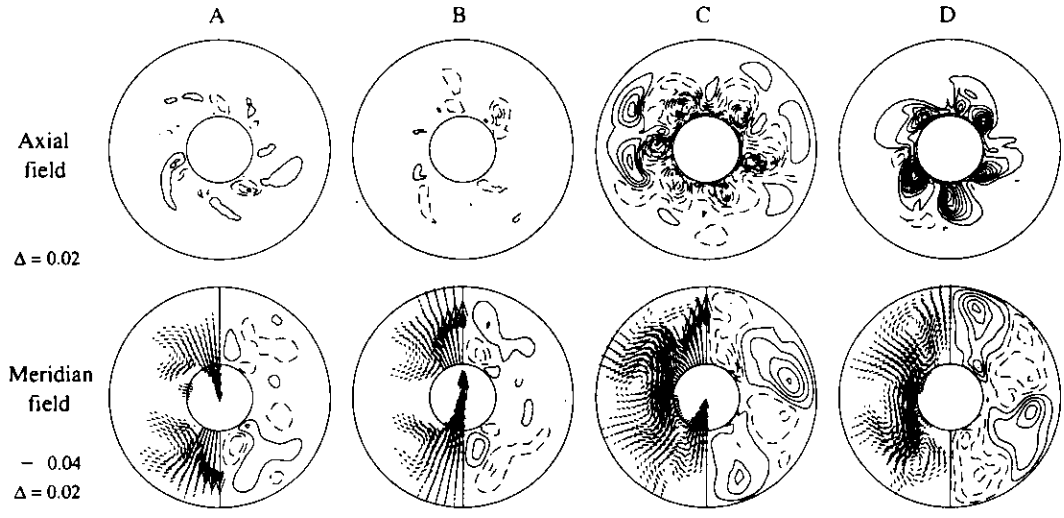

Figure 5.3: The magnetic field structures in two different energy states. Times A and B are in low energy states, and Times C and D in high energy states (The time positions of A, B, C, and D are marked by dashed lines in Figure 4.3 and Figure 4.9). Top row: the axial component of the magnetic field in the equatorial plane. Bottom row: the longitudinally averaged magnetic field in the meridian plane (left: poloidal vector; right: toroidal component.).

The convection columns drift in longitude about the axis of rotation. The number of convection columns and their drift directions are not fixed. In low energy states, the

convection columns drift westwards and keep almost unchanged structures. While in high energy states, they mainly drift eastwards and easily change their structures (as shown in Figure 4.7). As the convection columns do, the magnetic field pattern at the outer boundary is changing with time, and drifts eastwards in high energy states, and drifts westwards in low energy states.

In low energy states both of the convection columns and the radial component of magnetic field keep good structures. The convection motion is nearly symmetric around the equatorial plane, the fluid flow across the equatorial plane is very weak. So the axial component of the magnetic field is also very weak (as illustrated in Times A and B in the top row of Figure 5.3). The magnetic field line across the equatorial plane mainly go through the inner core (Times A and B in the bottom row of Figure 5.3).

While in high energy states, the convection motion is time-dependent, and the north-south symmetry of the convection pattern around the equatorial plane is broken, so there is a strong interaction of fluid flow between the northern and southern hemispheres. This strong interaction of fluid flow leads to the magnetic field lines across the equatorial plane by the aid of the convection columns (Times C and D in the bottom row of Figure 5.3).

It should be noted that the magnetic polarity changes are associated with the changes in toroidal field directions. It is clear the toroidal contour pattern of the longitudinally averaged magnetic field in the meridian plane is reversed as the dipole polarity is reversed (compare the right-hand sides of the bottom rows of Times A and B in Figure 5.3 and also of the Times C and D.).

5.3 Break of North-South Symmetry

From the discussions on the structures of the convection motion and the magnetic field in Sections 5.1 and 5.2, the importance of the north-south symmetry of the convection motion around the equatorial plane to the magnetic field reversals is very clear.

In low energy states, the thermal convection motion keeps its structure almost unchanged, and seven pairs of convection columns simply drift in longitudinal direction with relatively fast speed. There appear no flows across the equatorial plane (see the Times A and B of Figure 5.2), so the convection motion of the fluid generally is symmetric about the equatorial plane. The interaction of the flows in the north and south hemispheres is very weak. The magnetic field generated in this kind of convection motion with well-organized and almost unchanged convection motion pattern shows no polarity

reversal. The magnetic field is dipole-dominated structure. The dipole moment suffers only a small fluctuation in magnitude and direction.

In contrast, in high energy states, there arise relatively strong trans-equatorial flows (as one sees the Times C and D in the Figure 5.2). The basic columnar structure of the convection motion is vulnerable, and the number of convection column pairs (i.e., cyclone and anticyclone) changes between five to seven pairs. The existence of the strong trans-equatorial flows leads to the break of the symmetry of the convection pattern around the equatorial plane. The choice of the magnetic field structure is made to match the convection motion. So, the magnetic field shows strong axial component in the equatorial plane. Because of this symmetry break the columnar convection pattern in the spherical shell vessel becomes vulnerable. The nonlinear interaction of the fluid and the magnetic field makes it easy to change the direction of the trans-equatorial flows, furthermore influences the direction of the magnetic field. Thus, one can conclude that the generation of trans-equatorial flows in vortex columns must be the very clue to the reversal of the dipole field.

The most important discovery of these simulations is the generation of trans-equatorial flows in a spherical system that makes the convection pattern vulnerable and the whole system marginally stable, the reversal of the dipole magnetic field thereby being triggered occasionally and unexpectedly. We remind here that Sarson and Jones[55] and Sarson[56] have made an argument on the important of non-axisymmetric poloidal flow on the reversal.

5.4 Progress of A Magnetic Field Reversal

As an example of magnetic field reversals, we show in Figure 5.4 the snapshots of the structures of the convection columns and the magnetic field lines outside the spherical shell in a magnetic field reversal process happened around time = 79000. During this reversal, the convection motion changes rapidly. The north-south symmetry of the convection structure is greatly broken, and it leads to the change of convection motion in column number (as shown in Figure 4.7) and the change of magnetic field configuration. The magnetic field has a dominantly dipolar structure before (at time = 78482) and after (at time = 80028) the reversal, with the dipole axis nearly aligned with the rotation axis, which is vertical in Figure 5.4. During the polarity transition the magnetic field structure is much more complicated and the convection motion is constantly changing. With the change of the convection columns, the direction of magnetic dipole field varies,

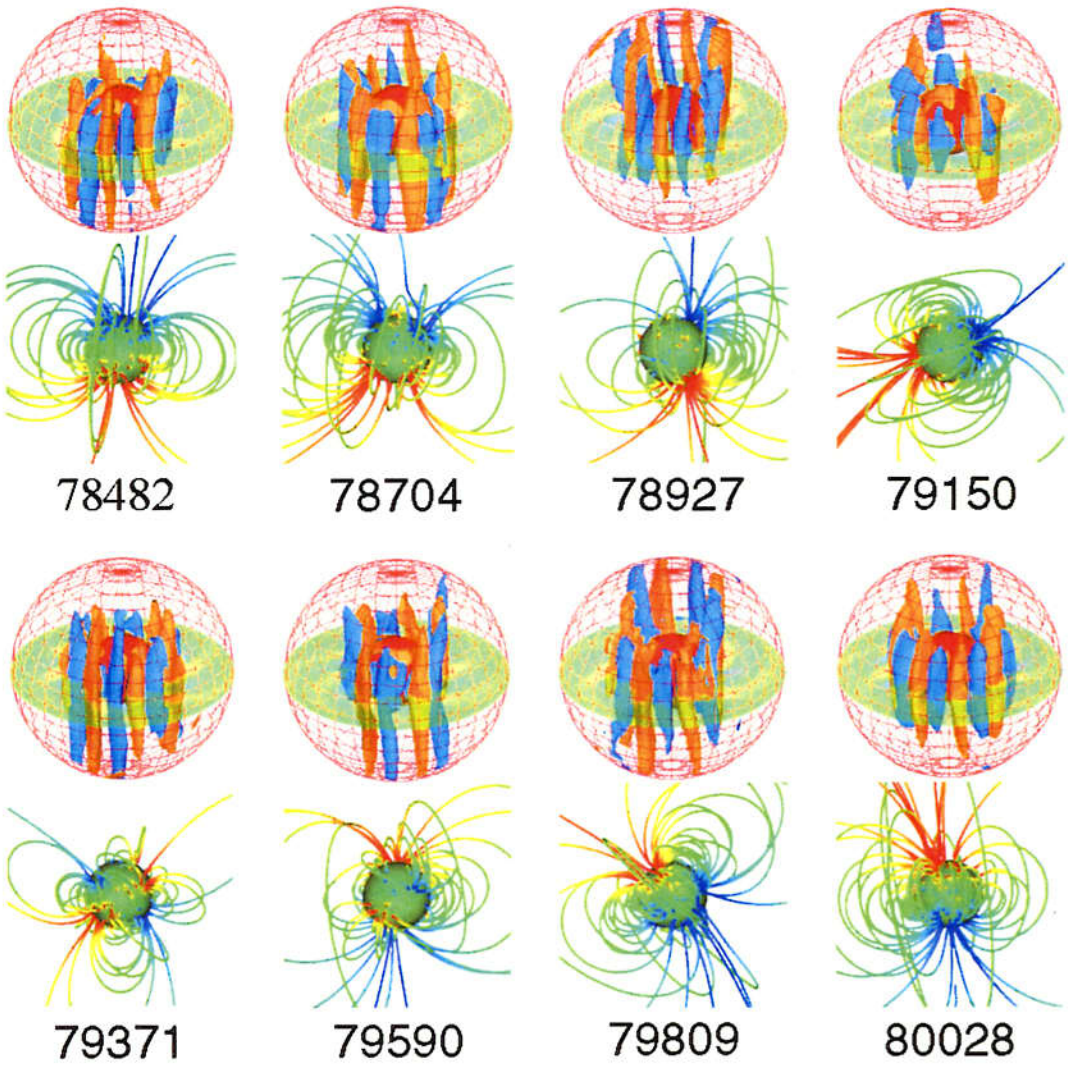

Figure 5.4: progress of a magnetic field reversal around time = 79000. Top row: the structure changes of convection columns (|axial vorticity| = 1, yellow for +1, blue for -1). Bottom row: the magnetic force lines outside the shell (its direction is from red to blue). The times are displayed at the bottoms.

the magnitude of dipole moment decreases and the quadrupole mode grows up. At time = 79371, the quadrupole mode becomes very strong (see Figure 5.4). At time = 79590, the dipole field becomes strong again. Finally at time = 80028, a complete magnetic field reverse is realized.

In this example of reversal, the growth of quadrupole mode before the reversal, the dominance quadrupole mode in the midway of the reversal, and the dominance of dipole mode after the reversal are shown clearly.

From this example of the magnetic field reversal, we can conclude that during a magnetic field reversal the structure of magnetic field goes from a dipole-dominated to a quadrupole-dominated, and finally recover its dipole-dominated structure when the magnetic field reverses its polarity completely.

Chapter 6

Interpretation of A Standard Run

A long time simulation has discovered that the magnetic dipolar field reverses its polarity repeatedly at irregular intervals. The time evolutions of total convection kinetic energy and generated magnetic energy make a flip-flop alternation between a high energy state and a low energy state. In low energy states, convection columns drift westward swiftly and keep almost unchanged structures, whereas in high energy states, they mainly drift eastward and easily change their structures. Dipole reversals occur only in high energy states.

6.1 Initial Phase

The fluid motions are driven by thermal convection. When the convection reaches a steady thermal convection state, it takes the form of convection columns regularly spaced round the axis of rotation and drifting in longitude. Figure 4.2 in Chapter 4 shows the velocity distribution and contours of density and axial component of vorticity in the equatorial plane. It is evident that there are five pairs of convection columns. After a random seed magnetic field is introduced to the system with steady thermal convection state, the magnetic field can develop through the dynamo action. Because in initial phase the Lorentz force is too weak to modify the convection greatly, the fluid keeps its convection motion pattern very well. As the magnetic field grows up, the Lorentz force becomes so strong that it can influence the convection motion. Due to the change of the convection motion, the growth of magnetic field will change according to the induction equation, and the magnetic field can not increase without a limit, or it will enter a high energy state in our standard simulation run. The change of convection motion (drifting motion of the

convection columns) is clearly shown in Figure 6.1). The dynamo simulation starts by introducing a seed magnetic field at time = 663, and the duration from time = 663 to about time = 2700 corresponds the initial phase.

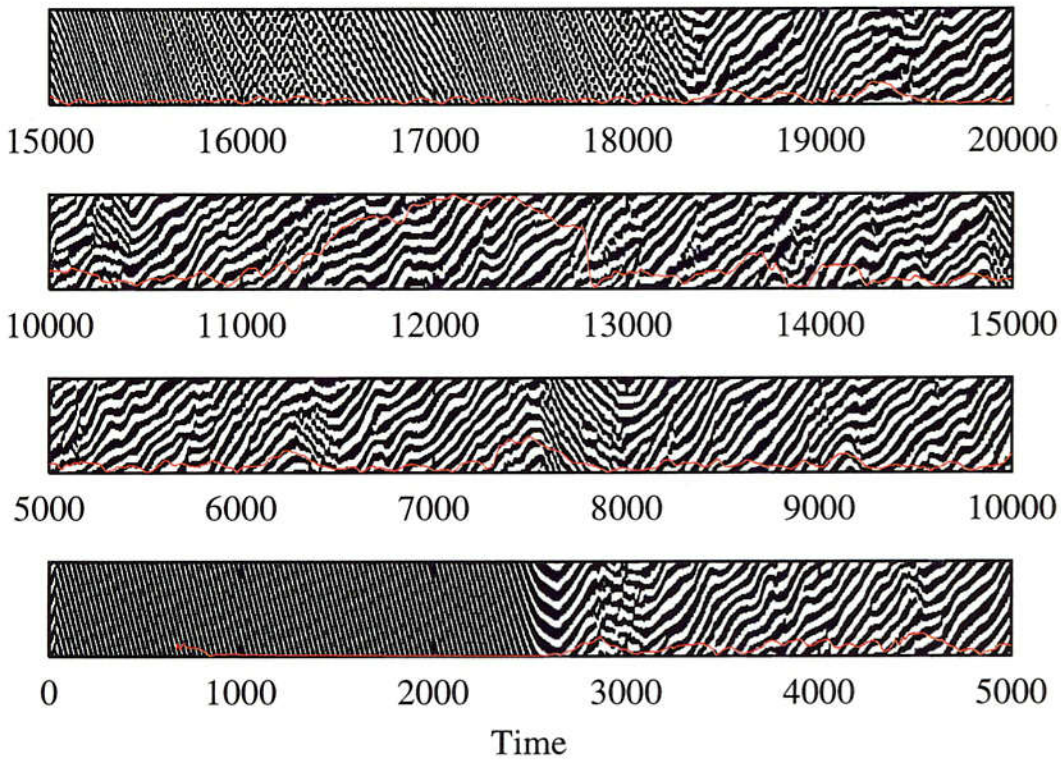

Figure 6.1: The drift motion of the convection columns in the equatorial for time = 0 – 20000. The horizontal axis is the time, and the vertical axis is the longitude ($0° \leq \phi \leq 360°$). The red line shows the pole latitude function with time.

6.2 Low Energy States

In our simulation result of standard run, low energy states are comparative steady, the thermal convection motion keeps its structure almost unchanged. There are seven pairs of convection columns drifting in longitude fast with nearly no changes in their flow patterns (top row in Figure 6.2). This kind of convection motion can maintain a magnetic field with dipole dominated structure at the outer boundary and the direction of dipole moment of

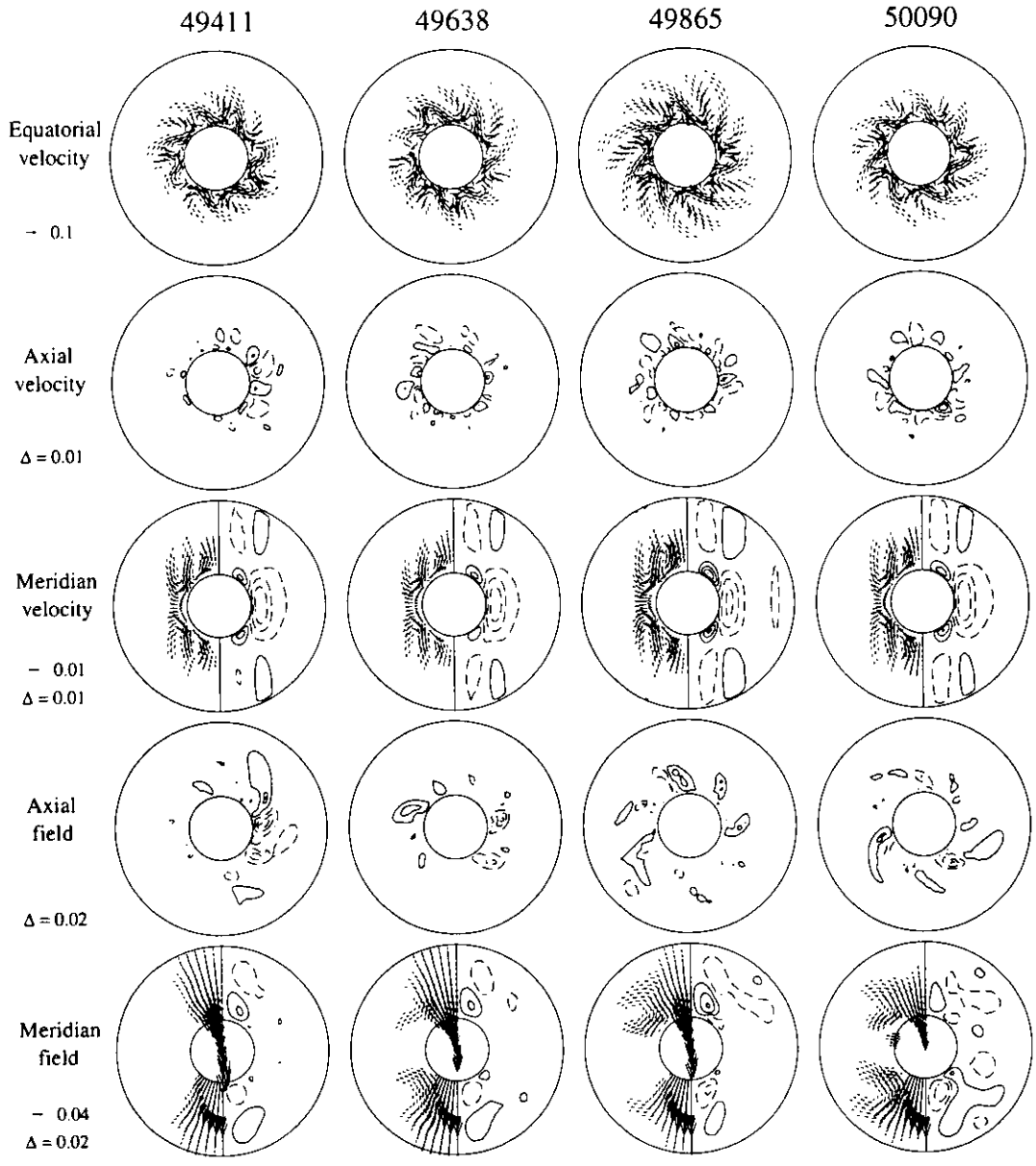

Figure 6.2: The velocity and magnetic field in a low energy state. Top row: velocity vector in the equatorial plane. Second row: axial velocity (contour map) in the equatorial plane. Third row: poloidal (left) and toroidal (right) components of the longitudinally averaged velocity in Meridian cross section. Fourth row: axial magnetic field (contour map) in the equatorial plane. Bottom row: poloidal (left) and toroidal (right) components of the longitudinally averaged magnetic field in Meridian cross section. The times are (from left to right): 49411, 49638, 49865, and 50090.

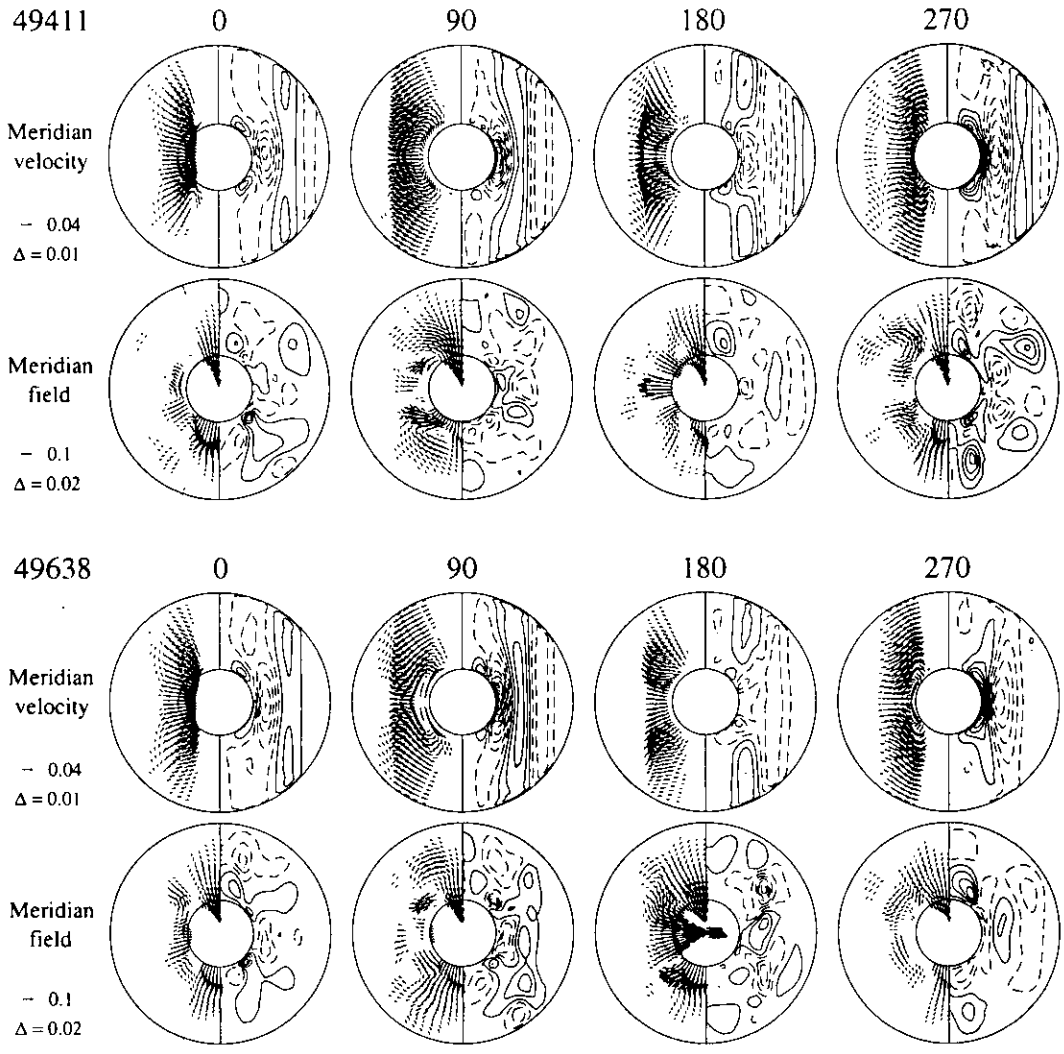

Figure 6.3: The meridian cross section distributions (longitude angle: 0°, 90°,180°, and 270°) of velocity (top row) and magnetic field (bottom row) in a low state. The meridional velocity and magnetic field are shown on the left-hand sides of these plots, and the azimuthal (zonal) components are shown as contour maps on the right-hand sides. The times are: 49411 and 49638.

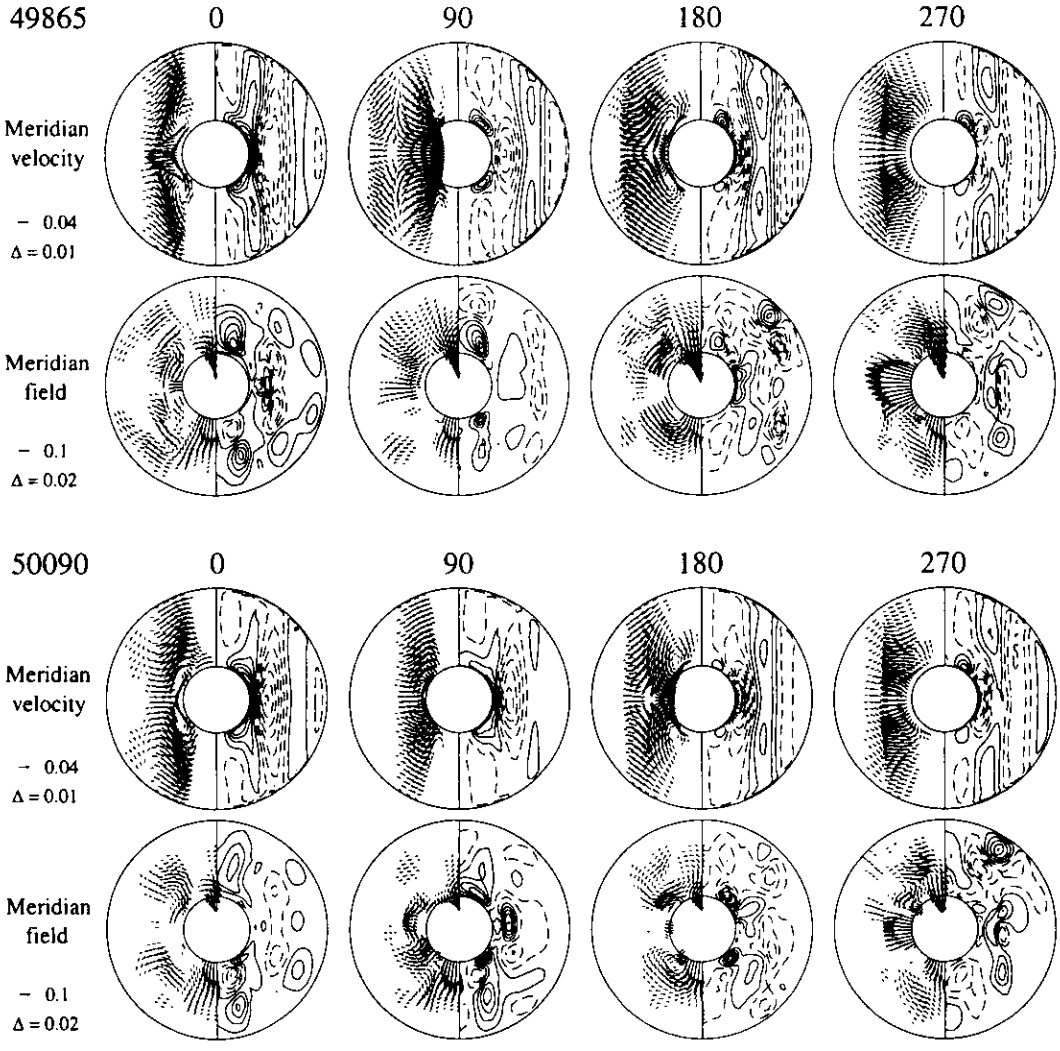

Figure 6.3 *(Continued)* The distributions of velocity and magnetic field in low energy state. The times are: 49865 and 50090.

the generated magnetic field is nearly parallel or anti-parallel to the rotation axis (refer to Figure 4.3 of Chapter 4). Some force balance exists in this energy state. The fluid motion shows a good north-south symmetry around the equatorial plane. The trans-equatorial flows, expressed by the axial components of velocity in equatorial plane, are very weak (the second row in Figure 6.2). The poloidal and toroidal components of the longitudinally averaged velocity in Meridian cross section shows the symmetry very clearly.

The magnetic field is generated by the convection motion of the electrically conducting fluid. Because of almost no change in the convection pattern, the magnetic force lines are expelled out of the convection columns, and then the magnetic field is mainly concentrated to the region of the tangent cylinder (the bottom row in Figure 6.2. The axial component of magnetic field in equatorial plane and longitude component of the longitudinally magnetic field in meridian plane are weak (the fourth and bottom rows in Figure 6.2). This result can be explained by the flux expulsion effect of MHD fluid when a band of eddies acts on a perpendicular magnetic field[76].

The meridian cross section distributions of velocity and magnetic field shown in Figure 6.3 provide their structure in more detail. The flow patterns of convection motions in every meridian cross sections clearly show good north-south symmetry. The flow in a cyclonic column is directed toward the equatorial plane; the flow in an anticyclonic column is directed away from the equatorial plane. It should be noted that near north and south polar regions there are no flows and magnetic field keeps its polarity very well (bottom rows in Figure 6.3). The low energy states are comparative steady, but the flows still show some very weak changes with time (top rows in Figure 6.3), which cause the changes of magnetic field (bottom rows in Figure 6.3).

Due to weak interaction of flows between the north and the south hemispheres, the convection motion keeps a good north-south symmetry around the equatorial plane, which makes it impossible for the magnetic field to reversal its polarity in low energy states. Therefore, the property of magnetic field in low energy states is that the magnetic field is dipolar dominated and the dipole moment shows small fluctuation in magnitude and keeps its polarity very well (refer to Figure 4.3 of Chapter 4).

6.3 High Energy States

The convection motion in high energy states exhibits the basic columnar structure, but it is highly time-dependent. Figure 6.4 is an example of an high energy state in which a reversal of magnetic field occurs with the dipole polarity changes from south-directed

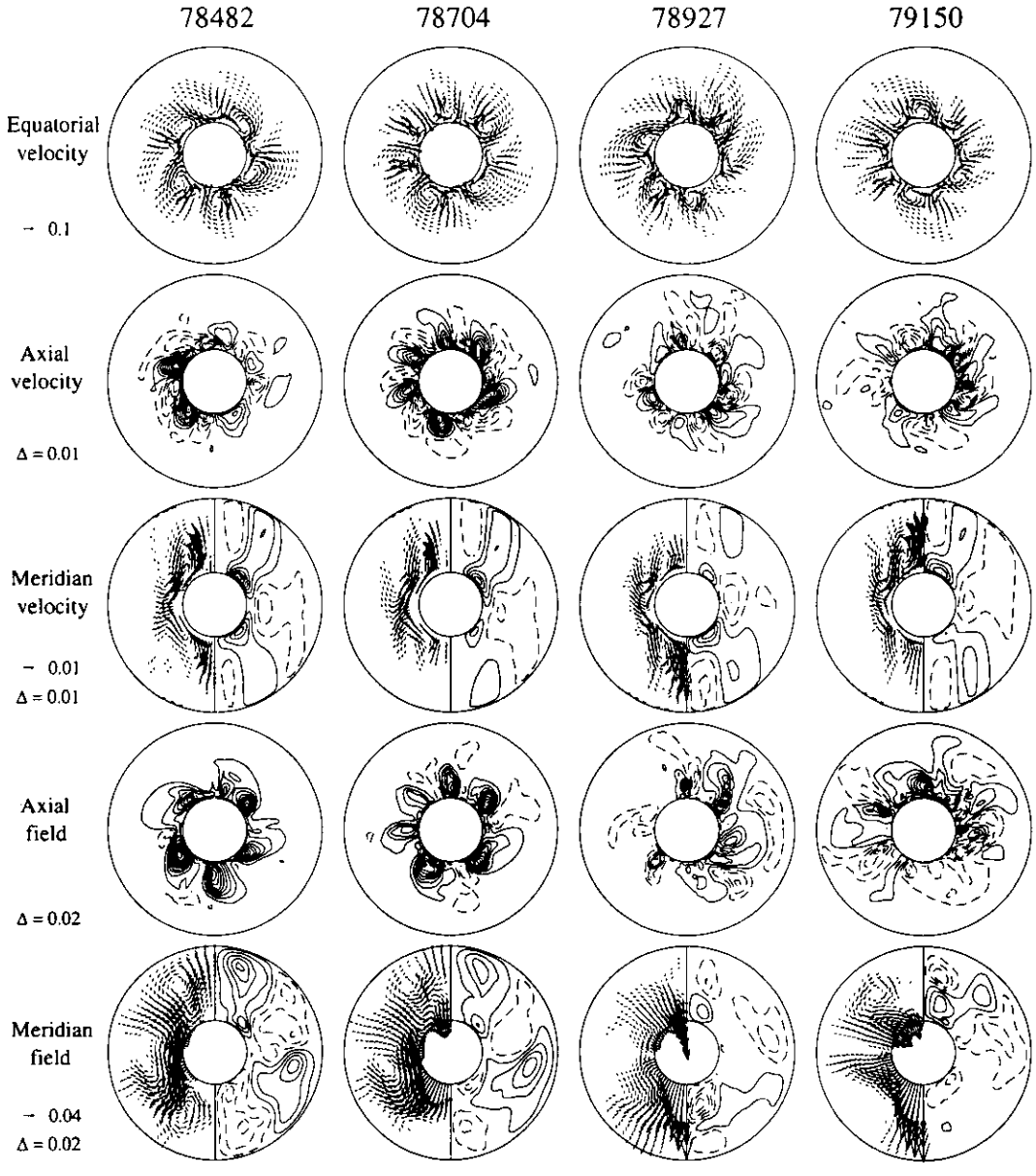

Figure 6.4: Same as Figure 6.2, but in a high energy state. The times are (from left to right): 78482, 78704, 78927, and 79150.

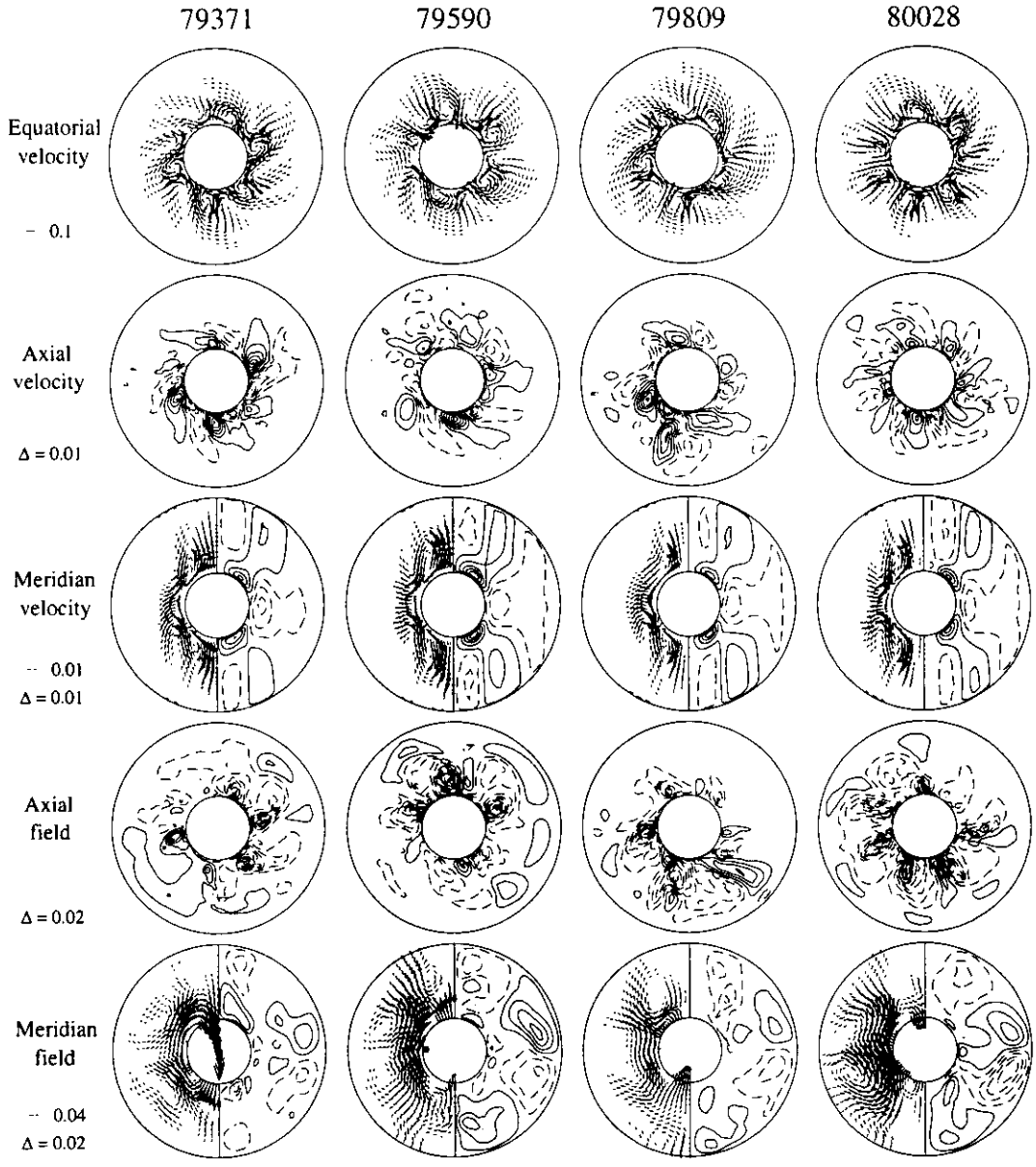

Figure 6.4 *(Continued)* The velocity and magnetic field in a high energy state. The times are (from left to right): 79371, 79590, 79809, and 80028.

to north-directed (refer to Figure 5.4). The number of convection column pair is not fixed, changing between five and seven pairs, and the structure of convection also keeps changing. The convection pattern can be seen in the velocity vector distribution in the equatorial plane (the first row in Figure 6.4). The number of the convection column is 5 pairs at time = 78482, 6 pairs at time = 78704, and 7 pairs at time = 80028.

Contrast to those in low energy states, the trans-equatorial flows in high energy states are strong (the second row of Figure 6.4). The north-south symmetry around the equatorial plane is broken. The distributions of fluid longitudinally averaged velocity in the meridian plane (the third row of Figure 6.4) clearly show the departure from equatorial symmetry of convection motion in the high energy states. The existence of the strong trans-equatorial flows in high energy states leads to the instability of the convection motion, and intensify the interaction of the convection motion between the north and south hemispheres. The flows near the north and south polar regions show some changes in their strengths with time (the third row of Figure 6.4), especially strong changes of the flows occur before the magnetic field reverses its polarity (times = 78927 and 79150).

It is well known that force lines of the magnetic field follow a perfectly conducting fluid in its motion. In a highly conducting fluid, the magnetic field has a tendency to become parallel or anti-parallel to the direction of the convection motion. In high energy states, the occurrence of trans-equatorial flows leads to intensification of magnetic field across the equatorial plane (the fourth row of Figure 6.4). The axial component of magnetic field in equatorial plane is strong in anticyclone convection columns (compare the first and the fourth rows of Figure 6.4). Before magnetic field reverses its polarity, the magnetic field shows the same direction in every anticyclone convection columns (time=78482, in the fourth rows of Figure 6.4). As time goes on, the magnetic field begins to change its direction in some convection columns (from time=78704 on in the fourth rows of Figure 6.4). Finally, the magnetic field directions in all anticyclone convection columns are reversed, and a magnetic field reversal process finishes (time=80028, the fourth rows of Figure 6.4).

The convection motions have basic columnar structure in high energy states, so the generated magnetic field possesses dipole-dominated structure at the outer boundary. During this reversal, with the change of the convection pattern, the structure of magnetic field shows some changes. The poloidal and toroidal components of the magnetic field change their directions as the time goes on (the fourth row of Figure 6.4).

The flow patterns of convection motions in high energy state keep the basic properties of low energy states. The flow in a cyclonic (anticyclonic) column is directed toward

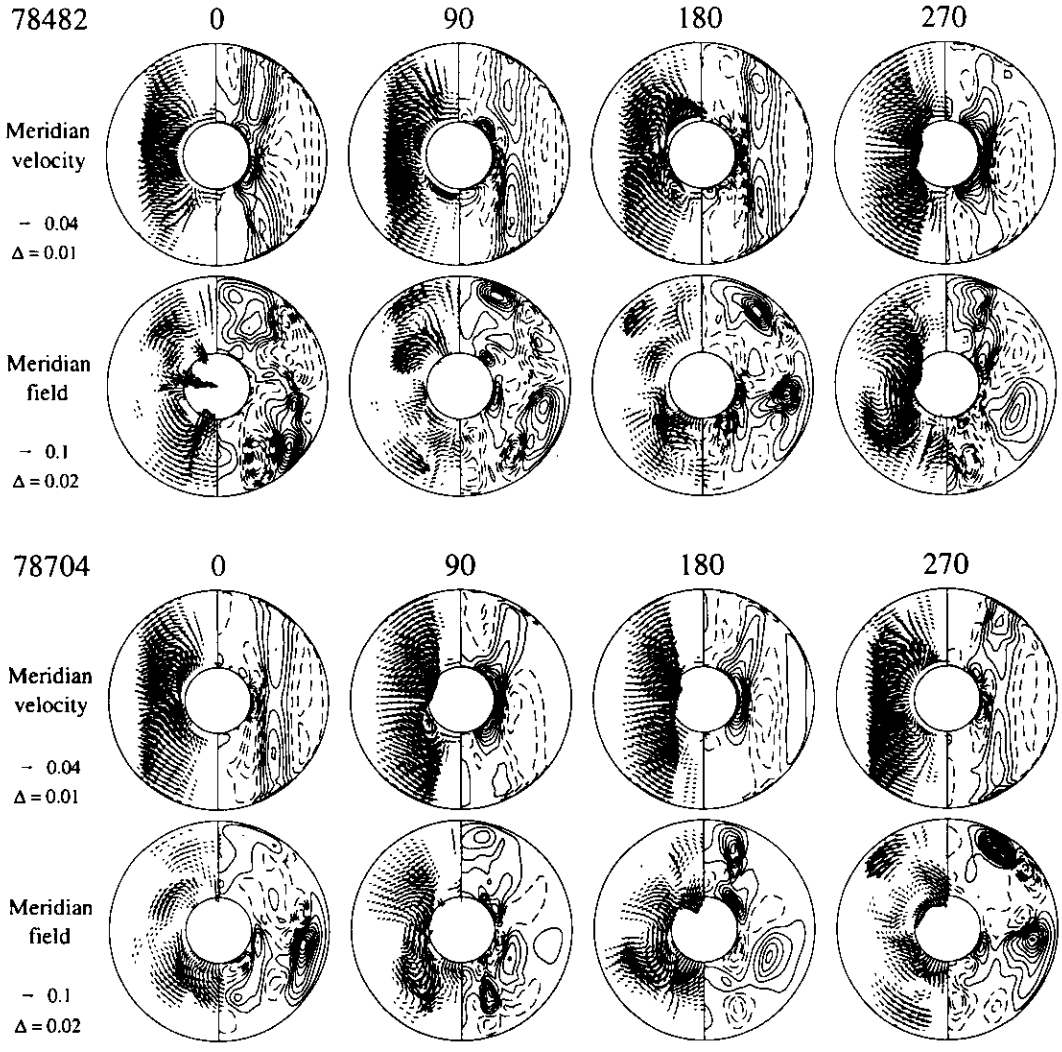

Figure 6.5: Same as Figure 6.3, but in a high energy state. The times are: 78482 and 78704.

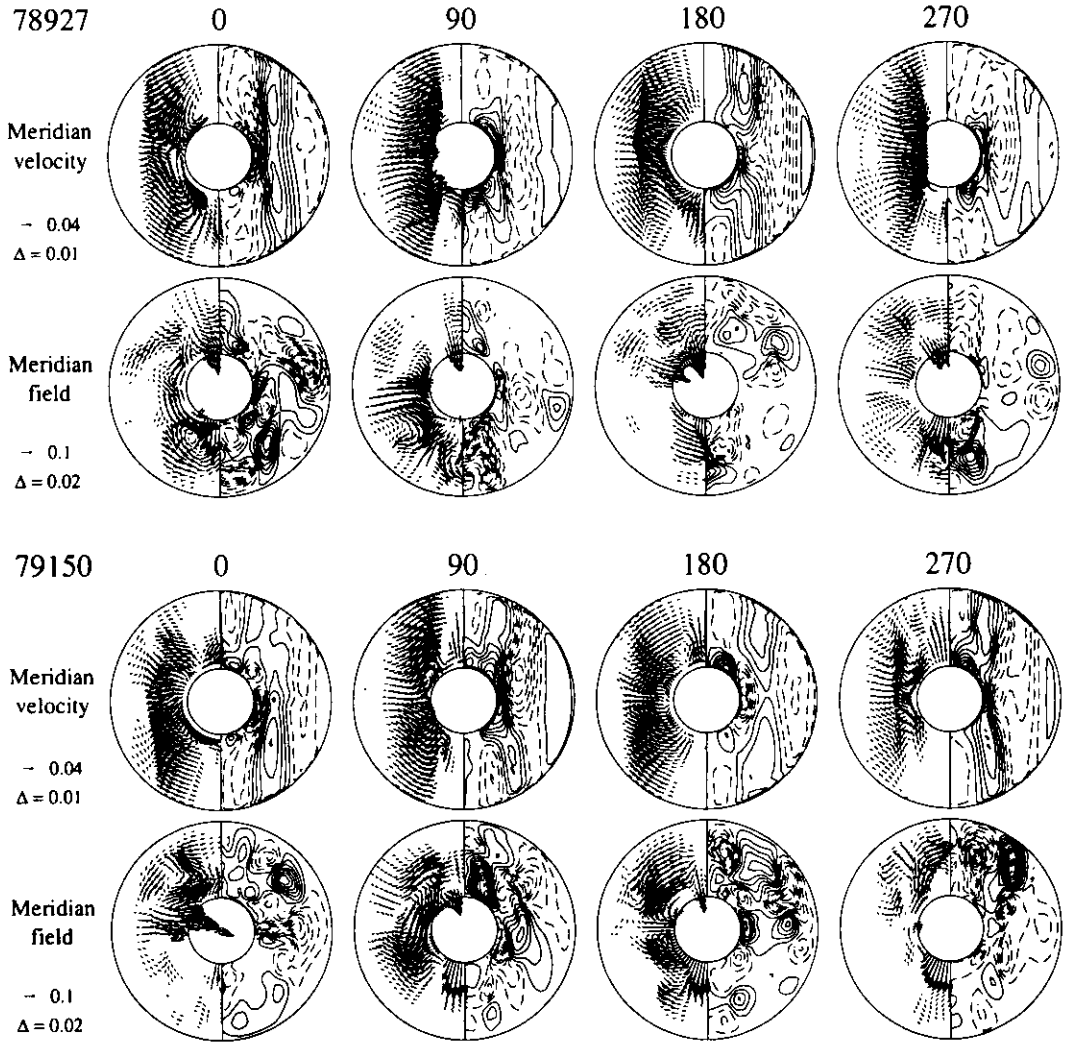

Figure 6.5 *(Continued)* The meridian cross section distributions of velocity and magnetic field in a high state. The times are: 78927 and 79150.

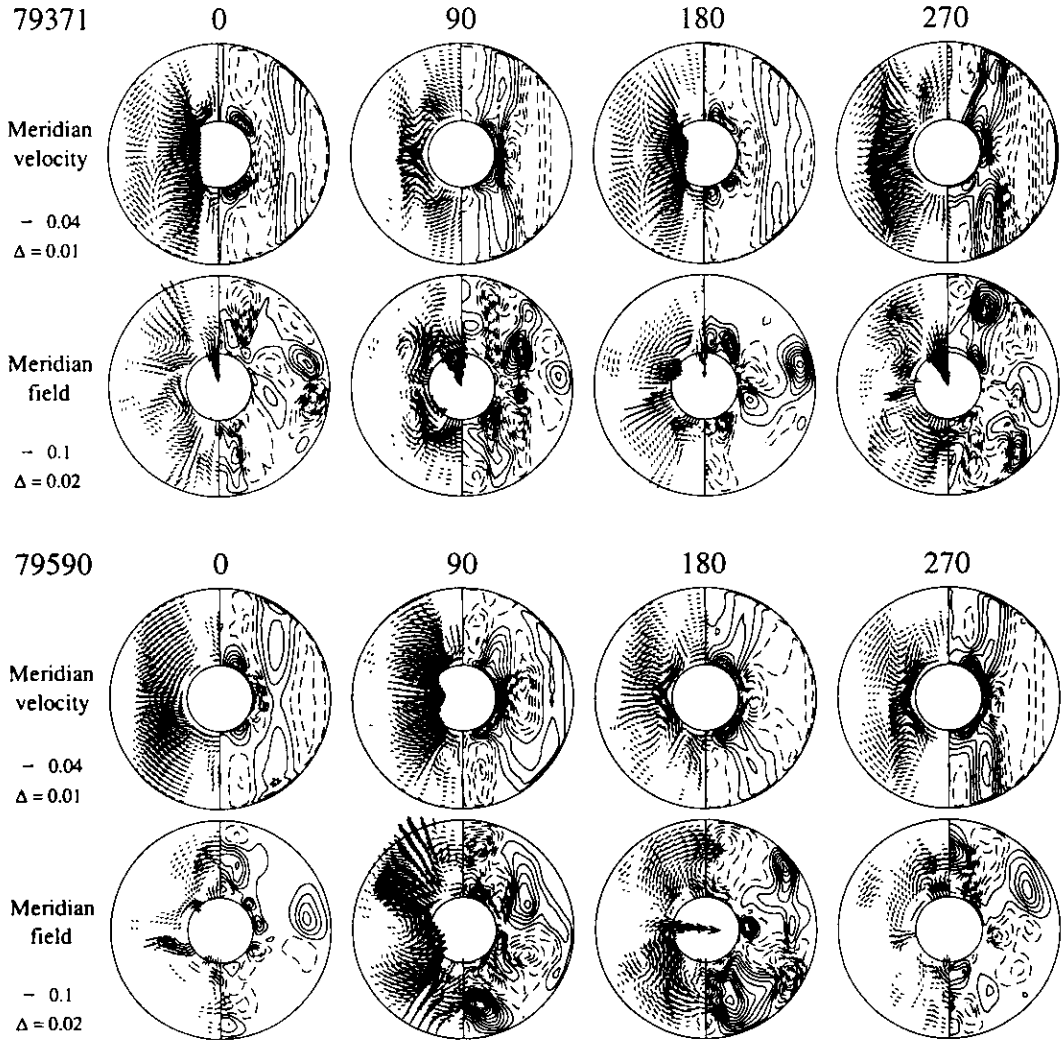

Figure 6.5 *(Continued)* The meridian cross section distributions of velocity and magnetic field in a high state. The times are: 79371 and 79590.

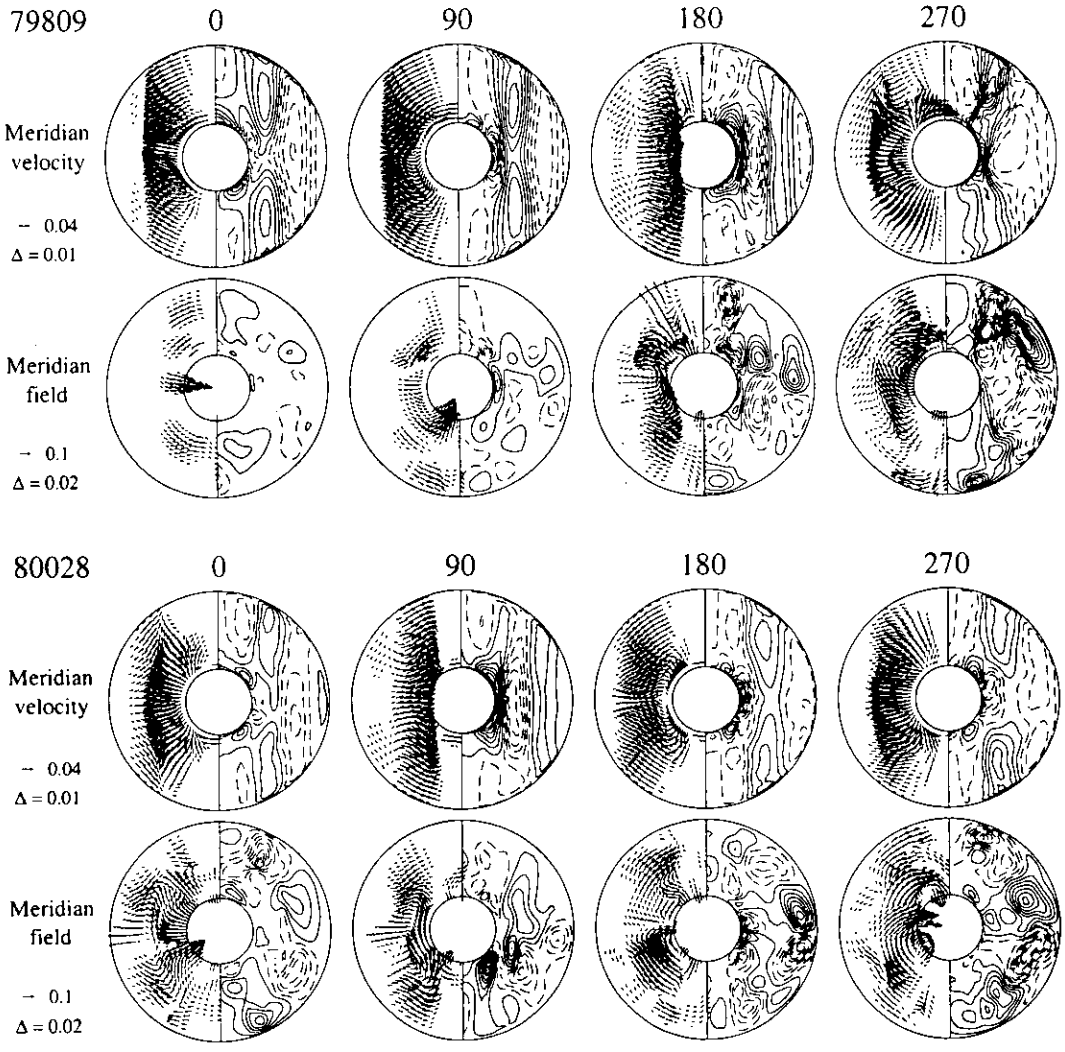

Figure 6.5 *(Continued)* The meridian cross section distributions of velocity and magnetic field in a high state. The times are: 79809 and 80028.

(away from) the equatorial plane (top rows in Figure 6.5). However, it should be noted that the flows near the north and south polar regions in high energy states (top rows in Figure 6.5) are quite different from those in low energy states (top rows in Figure 6.3). In high energy states, there exist flows across the polar regions, especially during a magnetic field reversal, which cause the changes of magnetic fields around the polar regions and furthermore the whole region.

In summary, the basic columnar structure of the convection motion in high energy states can maintain a dipole dominant magnetic field on the outer boundary. Due to the high time-dependence of the convection motions, the dipole moment of magnetic field shows some variations in its direction and magnitude. The strong trans-equatorial flows break the symmetry of fluid velocity field around the equatorial plane and strengthen the interaction of fluids in north and south hemispheres. These flows can help to initiate a magnetic field reversal unexpectedly and irregularly.

6.4 Others

In MHD dynamo theory, strong interaction of fluid motion and magnetic field, especially the interaction between the Coriolis and Lorentz forces, and strong nonlinearity of the MHD dynamo equations make it difficult to study the dynamo problem analytically.

Until now, the numerical simulation results of our standard run have provided some good interpretations to the convection motions and magnetic field behaviors in both high energy states and low energy states. However, some problems, such as the energy alternations between a high energy state and a low energy state, still remain unsolved.

The future work should be to find out the reason to existence of two kinds of energy states.

Chapter 7

Two Parameter Effects to Magnetic Field Reversal

In this Chapter, the effects of the electrical resistivity and the temperature difference between the inner and outer boundary to the generation and reversal of the magnetic field are discussed.

7.1 Effect of Electrical Resistivity

In MHD dynamo, generally the magnetic Reynolds number should be larger enough to maintain the dynamo action. We can change it by the electrical resistivity of the conducting fluid. Here we shall consider the possible effect of the electrical resistivity to the generation and reversal of the magnetic field.

We choose five different electrical resistivities η: Cases (1) 4.0×10^{-4}, (2) 3.0×10^{-4}, (4) 2.7×10^{-4}, (5) 2.5×10^{-4}, and (6) 1.0×10^{-4}. The other parameters are shown in Table 3.1 of Chapter 3. The dynamo simulations of these five cases start from the same steady thermal convection motion state, in which the velocity distribution and density contour in the equatorial plane keep almost unchanged westward-drifting patterns at constant angular velocity with 5 pairs of convection columns shown in Figure 4.1 and Figure 4.2.

To find similarities as well as differences of the five cases, we shall show the evolution of magnetic and kinetic energies, dipole moment, and the mean magnetic energy density on the outer boundary.

First, we show the time evolution of total convection kinetic energies and magnetic energies in Figure 7.1. At the beginning stages, the generated magnetic field in any one of all five cases is too weak to modify the convection motion. This is so-called kinematic dynamo region, in which the magnetic energy grows exponentially in time. According to the magnetic induction equation (1.8), as the electrical resistivity decreases, the magnetic field grows up quickly. This point can be seen clearly in Figure 7.1. The magnetic energy in Case (1) grows slowly, while the magnetic energy in Case (6) grows fast. The magnetic field generation mechanism has been clarified in Reference [42]. With the increase of magnetic field, the nonlinear magnetic (Lorentz) force becomes strong and influences the convection motion. The generated magnetic field gradually enters saturation region, and the generated magnetic energy exceeds the kinetic energy in all five cases.

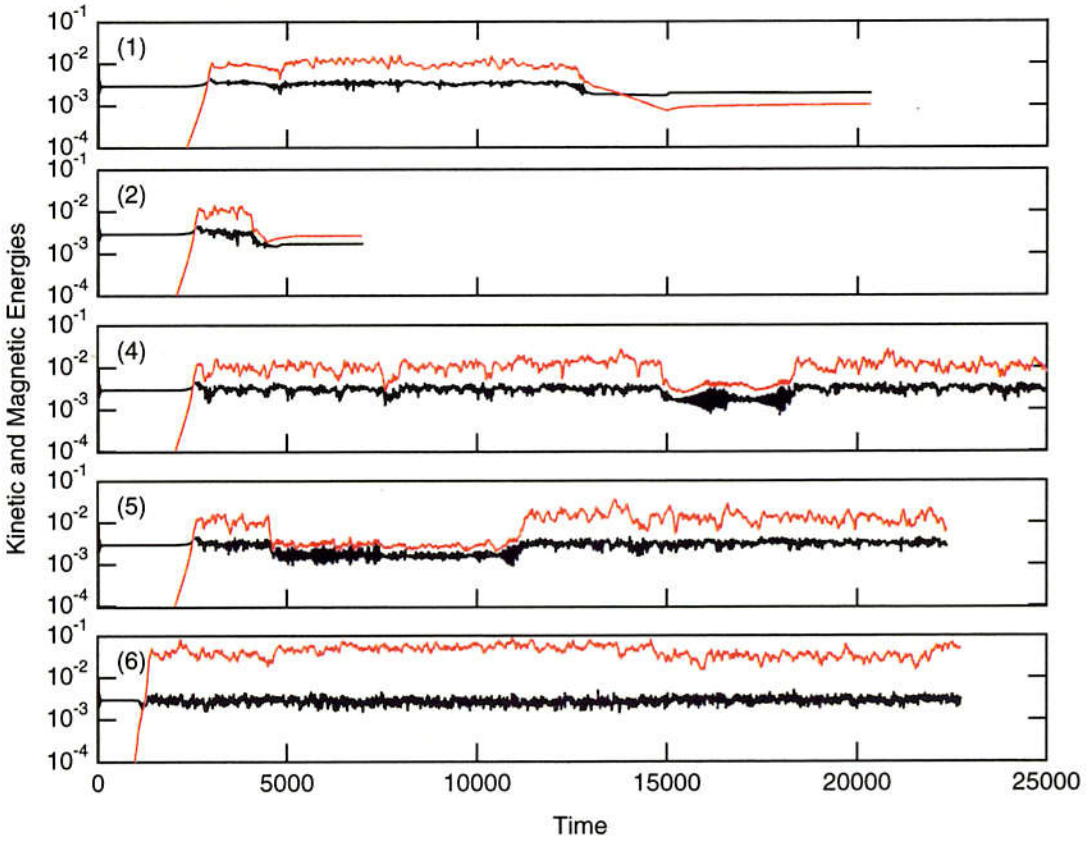

Figure 7.1: Time evolution of total convection kinetic energies (black lines) and magnetic energies (red lines) for electrical resistivity $\eta(\times 10^{-4})$: (1) 4.0, (2) 3.0, (4) 2.7, (5) 2.5, and (6) 1.0.

After the magnetic field saturates, the behaviors of the magnetic and kinetic energies show some differences related to the electrical resistivity. When the electrical resistivity is high, In Cases (1) and (2), the systems finally develop to low energy states in which both kinetic energy and magnetic energy show no fluctuations. No fluctuation of the final low energy states in Cases (1) and (2) means that the states are steady. In Case (1), the magnetic energy at final stage is lower than the kinetic energy in strength, while, in Case (2) the magnetic energy is higher than the kinetic energy.

In Cases (4) and (5), it is clear that there are two energy states for both kinetic energy and magnetic energy. The dynamo systems make flip-flop alternation between two energy states. The magnetic energy in a low energy state is almost the same order as the kinetic energy in a high energy state. In both energy states, the kinetic energy and magnetic energy fluctuate.

Case (6) shows a picture different from any one of other cases. There is only one high energy state for the total kinetic energy and magnetic energy. The total kinetic energy keeps nearly same level, although there are some fluctuations in magnitude. Meanwhile the magnetic energy sometime show a little decrease in magnitude.

Among these fives cases, the average generated magnetic energy in high energy states become high. As the electrical resistivity decreases, the average magnetic energy in high energy states becomes strong. The generated magnetic energy in Case (1) is the lowest, and that in Case (6) the highest.

Now, we shall consider the evolution of dipole field. Figure 7.2 shows the time evolution of magnetic dipole moment in these five cases. It should be mentioned that a different scale is used for the magnitude of dipole moment in Case (6). The magnetic polarity, or the direction of dipole moment, is expressed in pole latitude. The magnetic energies generated in Cases (1) and (2) are the weakest (as shown in figure 7.1), the dipole fields keep their polarities very well. No magnetic field reversals occur in these two cases. At the final stages, the dipole moments show no fluctuations in strength, as both the kinetic energy and magnetic energy do.

The magnetic field reverses its polarity in the other three cases. By comparison with Figure 7.1, we can find that the reversals occur only in the high energy states, which are shown in Cases (4), (5) and (6) of Figure 7.2. Cases (4) and (5) show some similarity. Their dipole moments in low energy states show smaller fluctuation in strength than they do in high energy states. The strongest dipole moment is generated in Case (6), which has the weakest electrical resistivity in the fives cases. It appears that it is difficult for the magnetic field to change its polarity when the dipole moment is strong, and that

the magnetic field reversals occur when dipole moment is weak, as shown in Case (6) of Figure 7.2.

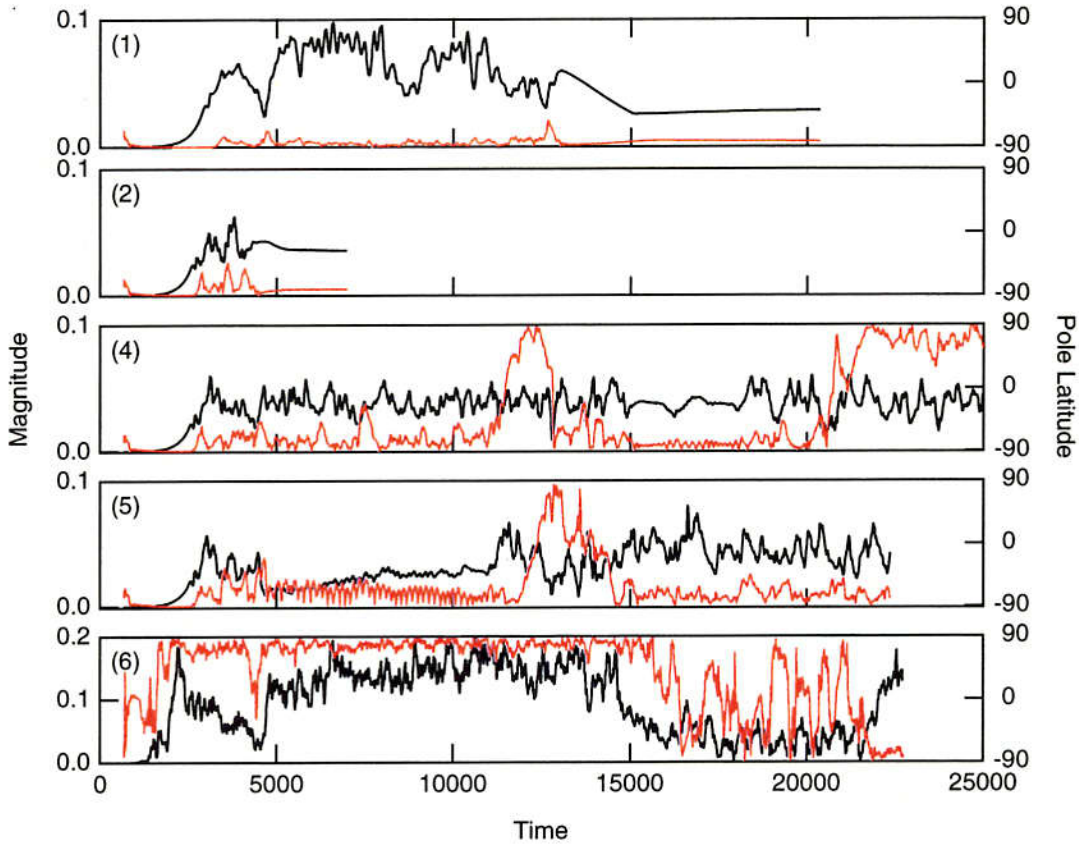

Figure 7.2: Time evolution of dipole moment for electrical resistivity $\eta(\times 10^{-4})$: (1) 4.0, (2) 3.0, (4) 2.7, (5) 2.5, and (6) 1.0. Black lines represent dipole moment's magnitude, and red lines its direction in pole latitude.

In addition to the reversals of its polarity, the magnetic dipole moment also shows a precession (Figure 7.3). The precession is measured in degree, and its positive direction is eastward. At the beginning stage, the convection motion drifts westward at a constant angular velocity (reference to Figure 6.1). Because the generated magnetic field is very weak, the dipole moment makes a westward precession at the same constant angular velocity with the convection motion. After magnetic energy saturates, the dipole moment shows different precession in each case. It can be seen clearly from the view of the dipole moment change that the magnetic energy saturates the earliest in Case (6) and the slowest in Case (1). In Cases (1) and (2), the dipole moments make eastward precession in high

energy states, and develop to the final stages with westward precession at constant angular velocities. In Cases (4) and (5), the dipole moments sometime precesses eastward, and sometime westward. In Case (6), the dipole moment keeps slow westward precession.

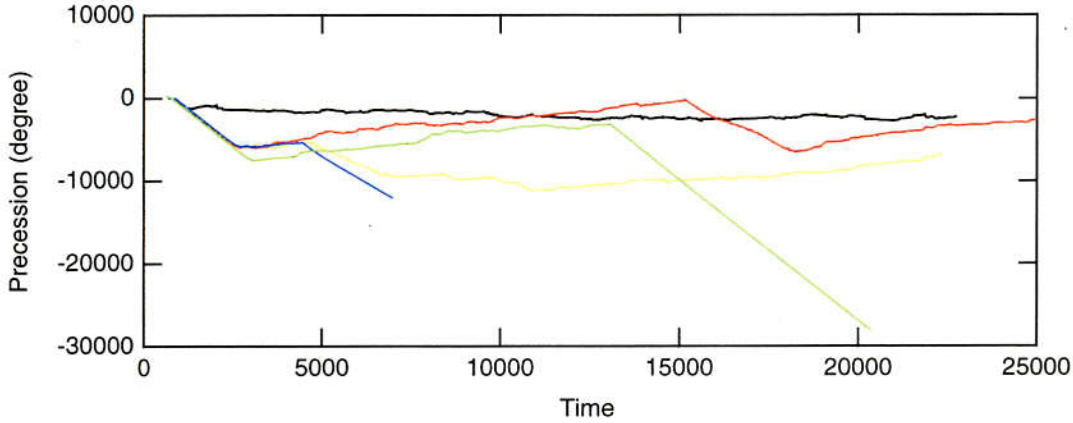

Figure 7.3: Precession of the dipole moment for different electrical resistivity $\eta(\times 10^{-4})$: (1) 4.0 (green), (2) 3.0 (blue), (4) 2.7 (red), (5) 2.5 (yellow), and (6) 1.0 (black).

Generally, the generated magnetic field in the spherical shell is much more complicated. However, the magnetic field at the surface of the outer boundary has a dominantly dipolar structure in most time of the simulation evolution. It can be understand by considering the mean magnetic energy density of the magnetic field on the outer boundary of the spherical shell. Figure 7.4 shows the time evolution of the first three spherical harmonic modes, dipolar, quadrupolar and octupolar, on the outer boundary (Note: different scales are used for the mean magnetic energy density.). In any one of the five cases, it appears that the dipole mode is larger than the others in most time of the simulation time, which means that the generated magnetic field is dipole dominated. The dynamo systems in Cases (1) and (2) finally reach to steady states, so their spherical harmonic modes keep no changes. For the dipole reversal cases of (5), (6), and (7), it is shown clearly in Figure 7.4 that the magnetic field easily reverses its polarity in high energy states when the quadrupolar mode is stronger than dipolar one. The reversals satisfy the conditions of the magnetic field reversal, which are given in Section 4.5.

In Cases of (1) and (2), the revolutions of energy, dipole moment and mean magnetic energy density on the outer boundary strongly confirm that the systems finally develop to stable states in which there exists some force balance.

The above results show that the electrical resistivity has great influence not only to the generation of magnetic field but also to the magnetic dipole reversal.

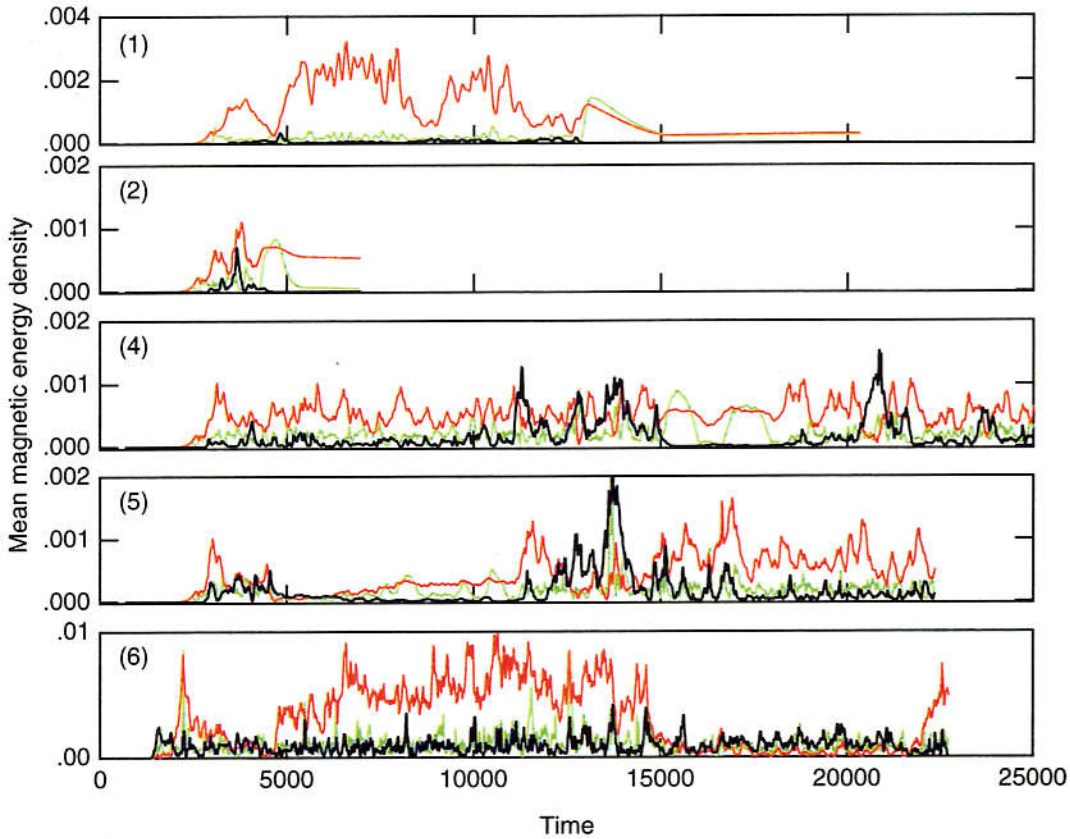

Figure 7.4: Mean magnetic energy densities of the first three spherical harmonic modes, dipolar (red), quadrupolar (black), and octupolar (green), at the outer boundary as a function of time for electrical resistivity $\eta(\times 10^{-4})$: (1) 4.0, (2) 3.0, (4) 2.7, (5) 2.5, and (6) 1.0.

7.2 Effect of Temperature at Inner Boundary

For the convection-driven dynamo in a rotating spherical shell, we can change the strength of the thermal driving by changing the temperature difference of inner and outer boundaries. To study the effects of inner boundary temperature to the generated magnetic field, we have carried out three dynamo simulations with different temperatures of the inner

boundary, Cases (7) $T_i = 3.5$, (8) $T_i = 5.0$, and (9) $T_i = 8.0$. The other parameters are shown in Table 3.1.

In the time evolution of total convection kinetic energy and generated magnetic energy shown in Figure 7.5, the magnetic energy shows bigger fluctuation than that at low rotation case. As the temperature at inner boundary increases, the thermal convection becomes strong, so the kinetic energy increases. This point can be clearly seen in the figure. In these three cases, the kinetic energy in Case (7) is the lowest, and the highest in the Case (9). The strong convection can generate high magnetic field and also causes the magnetic field to change a lot. In all three cases, dipole reverses its polarity frequently (as shown in Figure 7.6).

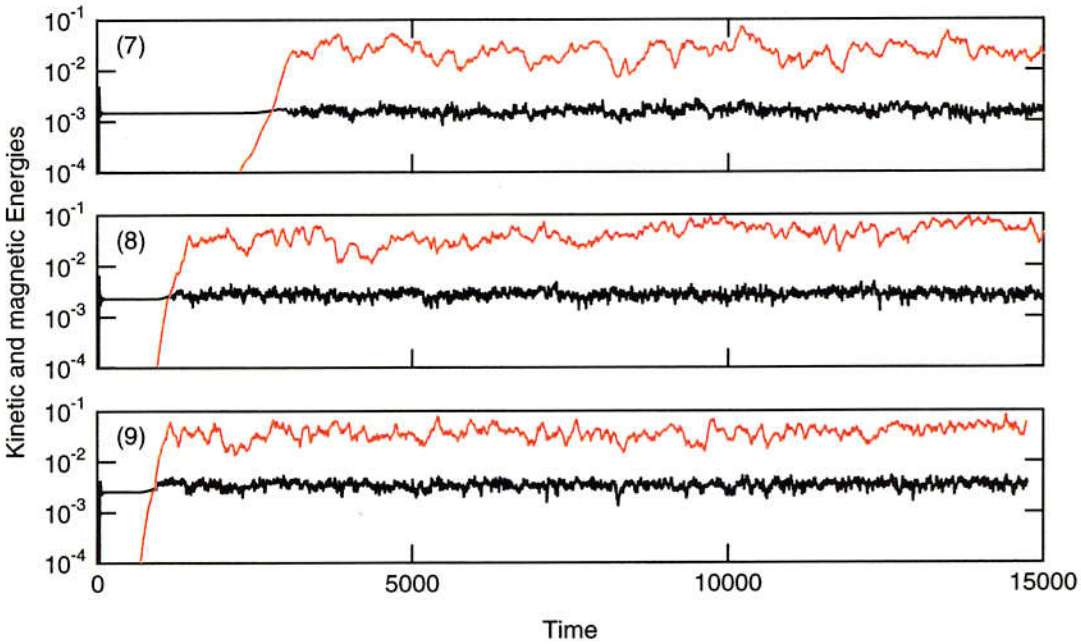

Figure 7.5: Time evolution of total convection kinetic energies (black lines) and magnetic energies (red lines) for inner boundary temperature T_i: (7) 3.5, (8) 5.0, and (9) 8.0.

In the time evolution of the mean magnetic energy densities of the first three spherical harmonic modes at the outer boundary shown in Figure 7.7, it is evident that the dipolar mode of magnetic field at outer boundary is not dominant in most simulation time while it is dominant in low rotation velocity cases. In Case (8), the dipole moment shows two high peaks. The increment of convection motion leads to the increase of generated magnetic field and that the dipole mode loses its dominant position.

The influence of rotation velocity to the dynamo action can be understood by comparing the Cases (7) and (6) which share the same parameters except the rotation velocity. The rotation velocity in Case (7) is higher than that in Case (6). In Figure 7.1(6) and Figure 7.5(7), it is obviously that as the rotation velocity increases, the total convection energy in a steady thermal convection state before introducing a random seed magnetic field to the system decreases. This point means that rotation acts to inhibit convection. For the dynamo action, the increase of rotation velocity leads to the decreases of both the total convection energy and the total magnetic energy and big fluctuation in total magnetic energy. The magnetic field changes from dipolar dominant type to non-dipolar dominant type.

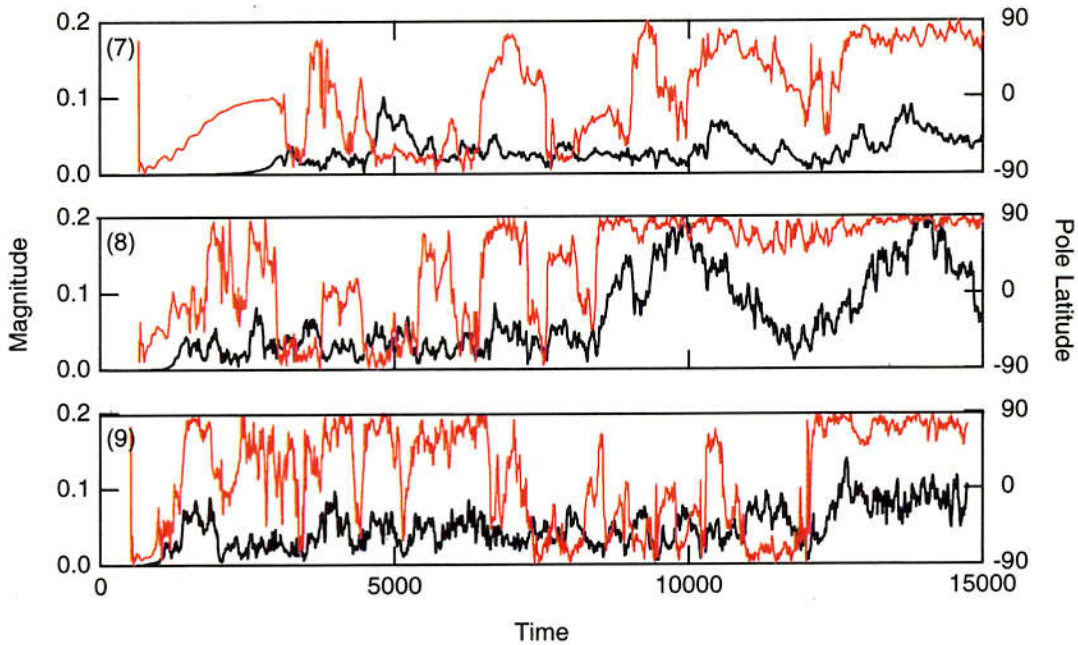

Figure 7.6: Time evolution of dipole moment for inner boundary temperature T_i: (7) 3.5, (8) 5.0, and (9) 8.0. Black lines represent dipole moment's magnitude, and red lines its direction in pole latitude.

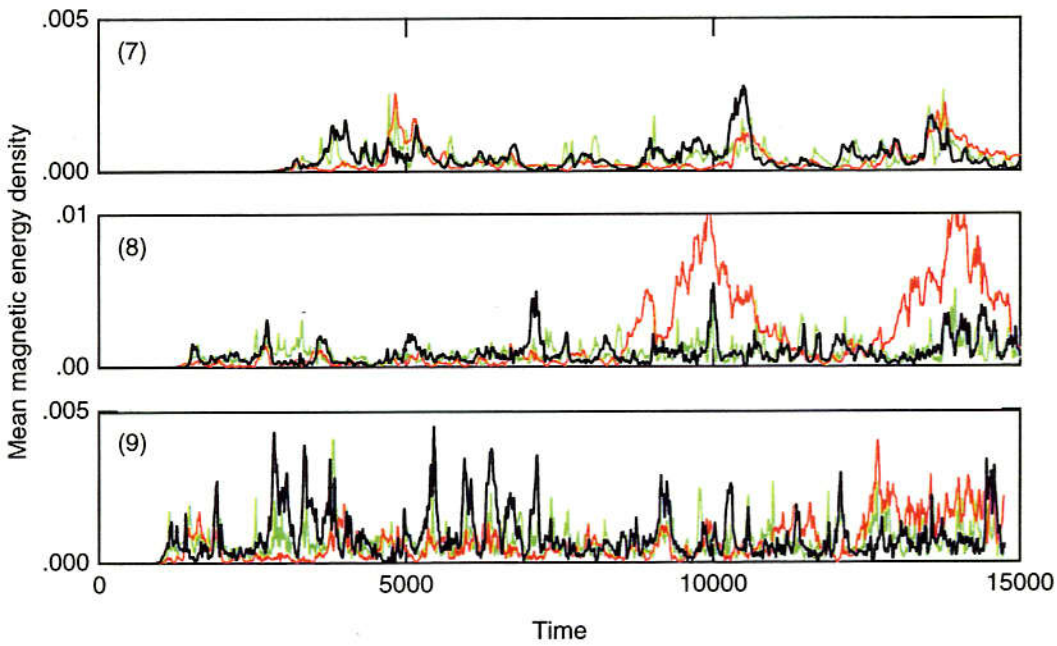

Figure 7.7: Mean magnetic energy densities of spherical harmonic modes, dipolar (red), quadrupolar (black), and octupolar (green), at the outer boundary as a function of time for inner boundary temperature T_i: (7) 3.5, (8) 5.0, and (9) 8.0.

Chapter 8

Conclusions and Summary

To understand the physical mechanism by which the magnetic field reverses its polarity, eight sets of physical parameters have been used to investigate the three dimensional convection-driven dynamo by Kageyama-Sato MHD dynamo model. A long duration, three-dimensional MHD simulation result of standard run has been successful in realizing a dominantly dipolar magnetic field which reverses polarity repeatedly and irregularly (i.e., punctuated reversal). The generated magnetic field has a strongly dipole dominated structure outside the spherical shell in most time of evolution. This is the first time for Kageyama-Sato model to observe repeated and sudden magnetic field reversals. The reversal appears to occur without any regular rule. It does reverse suddenly and the reversal does continue endlessly. As a whole, it is unlikely that the existence of one polarity predominates over the other.

The thermal convection in the rapidly rotating spherical shell takes the form of columnar cells which are parallel to the rotation axis. The magnetic field structure inside the spherical shell is very complicated. Generally, the magnetic field lines spiral around the convection columns. Interestingly, in the whole evolution of our standard run, the total magnetic and kinetic energies exhibit a flip-flop alternation between a high energy state and a low energy state. The different energy states correspond to different magnetic field configurations and convection patterns. In low energy states, the convection columns drift westwards and keep almost unchanged structures. The convection motion in high energy states exhibits the basic columnar structure, but nevertheless it is time-dependent.

Based on the standard run, the magnetic field reversal is studied in details. From the analyze of the time evolution of magnetic field, we obtain the necessary conditions for the occurrence of a dipole reversal, as followings: (1) the system is in a high energy state,

(2) the high energy state lasts for a certain period, (3) the quadrupole mode is on the average in a growing phase, and (4) the magnitude of the quadrupole mode exceeds that of the dipole mode on the outer boundary. The last two conditions are consistent with the suggested correlations between field strengths and reversals[75].

The magnetic field is generated by the convection motion of the electrically conducting fluid. So the magnetic field pattern is strongly correlated with the fluid flow in the sphere shell. In low energy states, the axial component of fluid velocity in the equatorial plane (i.e., trans-equatorial flow) is very weak. The convection motion is symmetric around the equatorial plane. While in high energy states, the trans-equatorial component of fluid velocity in the equatorial plane is very strong. The north-south symmetry around the equatorial plane is broken. The existence of the trans-equatorial flows in high energy states suggest that there is a strong interaction of fluid motion between the northern hemisphere and the southern hemispheres. This strong interaction of fluid flow is likely to be tilt-unstable, consequently the magnetic field might be reversed.

The most important and crucial discovery of this thesis is the generation of trans-equatorial flows in a spherical system that make the convection pattern vulnerable and the whole system marginally stable, the reversal of the dipole magnetic field thereby being triggered occasionally and unexpectedly.

The effects of electrical resistivity and the temperature difference between the inner and outer boundary to the magnetic field reversals are also analyzed. We find that the electrical resistivity is one of important physical parameters to the generation and reversal of the magnetic field.

Parameter runs find that dynamo action is strongly dependent on electrical resistivity. When the electrical resistivity is high, the system develops to a stable state in which total kinetic and magnetic energies keep almost constant and dipole field does not reverse its polarity. In this case, the generated magnetic field possesses weak energy due to large loss rate of magnetic energy, and it can not greatly change the convection motion of the fluid through Lorentz force. Therefore, the magnetic field generated by the convection motion maintains its polarity very well. As the electrical resistivity decreases, the loss rate of magnetic energy become small, and the Lorentz force increases. The increased Lorentz force can modifies the convection motion, furthermore changes itself. In this case, the time evolutions of total convection kinetic energy and generated magnetic energy make a flip-flop alternation between a high energy state and a low energy state. At low energy states, convection columns drift westward swiftly and keep almost unchanged structures, whereas at high energy states, they mainly drift eastward and easily change their structures. The

magnetic field is dipole dominated. It reverse its polarity at irregular intervals. At high energy states, The convection motion is modified strongly by the Lorentz force, and it leads to the change of magnetic field. In the view of magnetic dipole moment, it shows bigger variation in strength than that at low energy states. This is the reason that dipole reversals occur only at high energy states. A long time simulation in our standard run has discovered that the magnetic dipolar field reverses its polarity repeatedly at irregular intervals and the system does not prefer in one polarity state rather than the other. A dipole reversal occurs easily when the mean energy density of quadrupolar component at out boundary is stronger than that of dipolar one. For small electrical resistivity, the generated magnetic field becomes considerably strong, and dipole reversals occur at a high magnetic energy state too.

The effects of inner boundary temperature to the generated magnetic field are also studied. As the temperature at inner boundary increases, the thermal convection becomes strong, so the kinetic energy increases. Fast rotation acts to inhibit convection. For the dynamo action, the increase of rotation velocity leads to the decreases of both the total convection energy and the total magnetic energy and big fluctuation in total magnetic energy. The magnetic field changes from dipolar dominant type to non-dipolar dominant type.

Finally, it should be noted that the previous simulation[44] of Kageyama-Sato model, where the field reversal occurred in accordance with energy transition, turns out to be a very rare case. In fact, we found that the previous reversal was only transient and the system eventually relaxed to a steady state.

To sum up, in our numerical simulations of MHD dynamo, we have observed repeated and sudden magnetic field reversals, and obtained the conditions for magnetic field reversal. Furthermore, we have studied the mechanism of the magnetic field reversals and come to the conclusion that the break of the north-south symmetry around the equatorial plane of convection motion will lead to the magnetic field reversal. Although the parameter region of the real Earth is far from our present one, we believe that the core mechanism of the dipole reversal must be a universal one, as is often the case for most phenomena in nature. So the core reversal mechanism could be the same as ours because the flow pattern is the only direct agency related to the magnetic field pattern.

Acknowledgments

I wish to express my gratitude to Professor Tetsuya Sato for his great patient and elaborate guidance based on his remarkable understanding in physics, especially in complex science. I have received many benefits from every discussion with him in this three-year PhD course life. Moreover, I wish to thank him for providing me with an opportunity to study MHD dynamo theory.

I am greatly indebted to Dr. Akira Kageyama for providing the MHD code for dynamo simulation, helping me understand the physics of dynamo theory, and giving many helps on computation and scientific visualization.

I am greatly indebted to Dr. Y. Tomita Dr. S. Ishiguro and Dr. S. Fujiwara for their kind helps in my research and life in Japan.

My thanks are also extended to Ms. S. Urushihara, Mr. K. Matsuura, Ms. K. Shimazaki, Ms. Y. Kokubu, and Ms. C. Kondo for their zealous helps in my staying in Japan.

I am indebted to all other members of Theory and Computer Simulation Center of National Institute for Fusion Science (NIFS) for their helps in my research and life.

Japanese Ministry of Education, Culture, Sports, Science and Technology, which supports my studying and staying in Japan, is also acknowledged. The numerical computation of this work is performed on the MISSION System (Man-machine Interactive System for SimulatION) at NIFS, Japan.

My appreciation is extended to Professor X. T. He, Professor Weiyan Zhang, Professor Tiechang Chang, and Professor Shao-ping Zhu in Institute of Applied Physics and Computational Mathematics, for their constant encouragements and supports.

Special thanks go to my wife, Ping Yu, and my son, Chenxi Li, for their constant mental supports.

Bibliography

[1] J. A. Jacobs, *Reversals of the Earth's Magnetic Field*, 2nd ed. (Cambridge University Press, Cambridge, 1994).

[2] R. T. Merrill, M. W. McElhinny, and P. L. McFadden, *The Magnetic Field of the Earth: Paleomagnetism, the Core, and the Deep Mantle* (Academic Press, San Diego, 1996).

[3] J. E. P. Connerney, Magnetic fields of the outer planets, J. Geophys. Res. **98**, 18659-18679 (1993).

[4] N. F. Ness, Intrinsic magnetic fields of the planets: Mercury to Neptune. Philos. Trans. R. Soc. London, Ser. A **349**, 249-260 (1994).

[5] J. Larmor, How could a rotating body such as the sun become a magnet? Rep. Brit. Assoc. Adv. Sci. 159-160 (1919).

[6] H. K. Moffatt, *Magnetic Field Generation in Electrically Conducting Fluids* (Cambridge University Press, Cambridge, 1978).

[7] F. H. Busse, Magnetohydrodynamics of the Earth's dynamo. Annu. Rev. Fluid Mech. **10**, 435-462 (1978).

[8] P. H. Roberts and A. M. Soward, Dynamo theory. Annu. Rev. Fluid Mech. **24**, 459-512 (1992).

[9] P. H. Roberts, Fundamentals of dynamo theory, *Lectures on solar and planetary dynamos*, 1-58 (Cambridge University Press, 1994).

[10] P. H. Roberts and G. A. Glatzmaier, Geodynamo theory and simulations. Rev. Mod. Phys. **72**, 1081-1123 (2000).

[11] B. A. Buffett, Earth's core and the geodynamo. Science **288**, 2007-2012 (2000).

[12] C. A. Jones, Convection-driven geodynamo models. Philos. Trans. R. Soc. London, Ser. A **358**, 873-897 (2000).

[13] T. Sato, and the Complexity simulation group, Complexity in plasma: From self-organization to geodynamo. Phys. Plasmas **3**, 2135-2142 (1996).

[14] J.-P. Valet, and L. Meynadier, Geomagnetic field intensity and reversals during the past four million years. Nature **366**, 234-238 (1993).

[15] M. T. Juárez, L. Tauxe, J. S. Gee, and T. Pick, The intensity of the Earth's magnetic field over the past 160 million years. Nature **394**, 878-881 (1998).

[16] Y. Guyodo, and J.-P. Valet, Global changes in intensity of the Earth's magnetic field during the past 800 kyr. Nature **399**, 249-252 (1999).

[17] J. S. Gee, S. C. Cande, J. A. hildebrand,K. Donnelly, and R. L. Parker, Geomagnetic intensity variations over the past 780 kyr obtained from near-seafloor magnetic anomalies. Nature **408**, 827-832 (2000).

[18] M. Kono, H. Tanaka, H. Tsunakawa, Spherical harmonic analysis of paleomagnetic data: The case of linear mapping. J. Geophys. Res. **105**, 5817-5833 (2000).

[19] P. David, Sur la stabilité de la direction d'aimantation dans quelques roches volcaniques. C. R. Acad. Sci. Paris **138**, 41-42 (1904).

[20] B. Brunhes, Recherches sur le direction d'aimantation des roches volcaniques. J. Phys. **5**, 705-724 (1906).

[21] T. G. Cowling, *Magnetohydrodynamics* (Interscience Publishers, New York, 1957).

[22] P. H. Roberts, *An Introduction to Magnetohydrodynamics* (Longmans, London, 1967).

[23] P. H. Roberts, Kinematic dynamo models, Phil. Trans. R. Soc. Lond. A **272**, 663-698 (1972).

[24] T. G. Cowling, The magnetic field of sunspots. Mon. Not. Roy. Astron. Soc. **94**, 39-48 (1934).

[25] S. Chandrasekhar, *Hydrodynamic and Hydromagnetic Stability* (Clarendon Press, Oxford, 1961).

[26] P. H. Roberts, On the thermal instabilities of a rotating-fluid sphere containing heat sources, Phil. Trans. R. Soc. Lond. A **263**, 93-117 (1968).

[27] B. H. Busse, Thermal instabilities in rapidly rotating systems, J. Fluid Mech. **44**, 441-460 (1970).

[28] D. R. Fearn, Hydromagnetic flow in planetary cores. Rep. Prog. Phys. **61**, 175-235 (1998).

[29] K. Zhang, and G. Schubert, Magnetohydrodynamics in rapidly rotating spherical systems. Annu. Rev. Fluid Mech. **32**, 409-443 (2000).

[30] P. A. Gilman and J. Miller, Dynamically consistent nonlinear dynamos driven by convection in a rotating spherical shell, Astrophys. J. Suppl. Ser. **46**, 211-238 (1981).

[31] P. A. Gilman, Dynamically consistent nonlinear dynamos driven by convection in a rotating spherical shell. II. Dynamos with cycles and strong feedbacks, Astrophys. J. Suppl. Ser. **53**, 243-268 (1983).

[32] G. A. Glatzmaier and P. H. Roberts, A three-dimensional convective dynamo solution with rotating and finitely conducting inner core and mantle. Phys. Earth Planet. Inter. **91**, 63-75 (1995).

[33] G. A. Glatzmaier and P. H. Roberts, A three-dimensional self-consistent computer simulation of a geomagnetic field reversal. Nature **377**, 203-209 (1995).

[34] G. A. Glatzmaier and P. H. Roberts, An anelastic evolutionary geodynamo simulation driven by compositional and thermal convection. Physica D **97**, 81-94 (1996).

[35] G. A. Glatzmaier and P. H. Roberts, Rotation and magnetism of Earth's inner core. Science **274**, 1887-1891 (1996).

[36] G. A. Glatzmaier, R. S. Coe, L. Hongre, and P. H. Roberts, The role of the Earth's mantle in controlling the frequency of geomagnetic reversals. Nature **401**, 885-890 (1999).

[37] W. Kuang, and J. Bloxham, An Earth-like numerical dynamo model. Nature **389**, 371-374 (1997).

[38] W. Kuang, and J. Bloxham, Numerical modeling of magnetohydrodynamic convection in a rapidly rotating spherical shell: Weak and strong field dynamo action. J. Comput. Phys. **153**, 51-81 (1999).

[39] G. R. Sarson, C. A. Jones, and A. W. Longbottom, Convection driven geodynamo models of varying Ekman number. Geophys. Astrophys. Fluid Dynamics **88**, 225-259 (1998).

[40] U. Christensen, P. Olson, and G. A. Glatzmaier, Numerical modeling of the geodynamo: a systematic parameter study. Geophys. J. Int. **138**, 393-409 (1999).

[41] A. Kageyama, T. Sato, and the Complexity simulation group, Computer simulation of a magnetohydrodynamic dynamo. II. Phys. Plasmas **2**, 1421-1431 (1995).

[42] A. Kageyama and T. Sato, Generation mechanism of a dipole field by a magnetohydrodynamic dynamo. Phys. Rev. E **55**, 4617-4626 (1997).

[43] A. Kageyama and T. Sato, Velocity and magnetic field structures in a magnetohydrodynamic dynamo. Phys. Plasmas **4**, 1569-1574 (1997).

[44] A. Kageyama, M. M. Ochi and T. Sato, Flip-flop transitions of the magnetic intensity and polarity reversals in the magnetohydrodynamic dynamo. Phys. Rev. Lett. **82**, 5409-5412 (1999).

[45] U. Christensen, P. Olson, and G. A. Glatzmaier, A dynamo model interpretation of the geomagnetic field structure. Geophys. J. Int. **138**, 393-409 (1999).

[46] P. Olson, U. Christensen, and G. A. Glatzmaier, Numerical modeling of the geodynamo: Mechanisms of field generation and equilibration. J. Geophys. Res. **104**, 10383-10404 (1999).

[47] S. Kida, and H. Kitauchi, Chaotic reversals of Dipole moment of thermally driven magnetic field in a rotating spherical shell. J. Phys. Soc. Jpn. **67**, 2950-2951 (1998).

[48] S. Kida, and H. Kitauchi, Thermally driven MHD dynamo in a rotating spherical shell. Prog. Theoretical Phys. Supp. **130**, 121-136 (1998).

[49] E. Grote, and F. H. Busse, Hemispherical dynamos generated by convection in rotating spherical fluid shells. Phys. Rev. E **62**, 4457-4460 (2000).

[50] R. Hollerbach, and C. A. Jones, Influence of the Earth's inner core on geomagnetic fluctuations and reversals. Nature **365**, 541-543 (1993).

[51] A. Sakuraba, and M. Kono, Effect of the inner core on the numerical solution of the magnetohydrodynamic dynamo. Phys. Earth Planet. Inter. **111**, 105-121 (1999).

[52] E. Grote, F. H. Busse, and A. Tilgner, Convection-driven quadrupolar dynamos in rotating spherical shells. Phys. Rev. E **60**, R5025-R5028 (1999).

[53] M. M. Ochi, A. Kageyama, and T. Sato, Dipole and octupole field reversals in a rotating spherical shell: Magnetohydrodynamic dynamo simulation. Phys. Plasmas **6**, 777-787 (1999).

[54] R. S. Coe, L. Hongre, G. A. Glatzmaier, An examination of simulated geomagnetic reversals from a palaeomagnetic perspective, Phil. Trans. R. Soc. Lond. A **358**, 1141-1170 (2000).

[55] G. R. Sarson, and C. A. Jones, A convection driven geodynamo reversal model. Phys. Earth Planet. Inter. **111**, 3-20 (1999).

[56] G. R. Sarson, Reversal models from dynamo calculations. Philos. Trans. R. Soc. London, Ser. A **358**, 921-942 (2000).

[57] F. H. Busse, Homogeneous dynamos in planetary cores and in the laboratory. Annu. Rev. Fluid Mech. **32**, 383-408 (2000).

[58] A. Tilgner, Towards experimental fluid dynamos. Phys. Earth Planet. Inter. **117**, 171-177 (2000).

[59] A. Gailitis, O. Lielausis, S. Dement'ev, E. Platacis, A. Cifersons, G. Gerbeth, T. Gundrum, F. Stefani, M. Christen, H. Hänel, and G. Will, Detection of a flow induced magnetic field eigenmode in the Riga dynamo facility. Phys. Rev. Lett. **84**, 4365-4368 (2000).

[60] N. L. Peffey, A. B. Cawthorne, and D. P. Lathrop, Toward a self-generating magnetic dynamo: The role of turbulence. Phys. Rev. E **61**, 5287-5294 (2000).

[61] A. Jackson, Critical time for fluid dynamos. Nature **405**, 1003-1004 (2000).

[62] A. Gailitis, O. Lielausis, E. Platacis, S. Dement'ev, A. Cifersons, G. Gerbeth, T. Gundrum, F. Stefani, M. Christen, and G. Will, Magnetic field saturation in the Riga dynamo experiment. Phys. Rev. Lett. **86**, 3024-3027 (2001).

[63] P. M. Gerhart, R. J. Gross, *Fundamentals of fluid mechanics*, p10, (Addision-Wesley Publishing Company, Tokyo, 1985).

[64] A. Kageyama, K. Watanabe, and T. Sato, Simulation study of a magnetohydrodynamic dynamo: Convection in a rotating spherical shell. Phys. Fluids B **5**, 2793-2805 (1993).

[65] H. Kitauchi, K. Araki, and S. Kida, Flow structure of thermal convection in a rotating spherical shell. Nonlinearity **10**, 885-904 (1997).

[66] G. D. Smith, *Numerical Solution of Partial Differential Equations: Finite Difference Methods*, 3rd ed. (Clarendon Press, Oxford, 1985).

[67] E. A. Spiegel, Convective instability in a compressible atmosphere. I. Astrophys. J. **141**, 1068-1090 (1965)

[68] J. B. Taylor, The magneto-hydrodynamics of a rotating fluid and the Earth's dynamo problem. Proc. R. Soc. Lond Ser. A **274**, 274-283 (1963).

[69] J. Li, T. Sato, and A. Kageyama, Repeated and Sudden Reversals of the Dipole Field Generated by a Spherical Dynamo Action, Science **295**, 1887-1890 (2002).

[70] K.-K. Zhang, and F. H. Busse, On the onset of convection in rotating spherical shells. Geophys. Astrophys. Fluid Dynamics **39**, 119-147 (1987).

[71] K. Zhang, Spiralling columnar convection in rapidly rotating spherical fluid shells. J. Fluid Mech. **236**, 535-556 (1992).

[72] F. H. Busse, Non-linear properties of thermal convection. Rep. Prog. Phys. **41**, 1929-1967 (1978).

[73] E. Grote, and F. H. Busse, Dynamics of convection and dynamos in rotating spherical fluid shells. Fluid Dyn. Res. **28**, 349-368 (2001).

[74] J. D. Jackson, *Classical Electrodynamics*, p65, (John Wiley & Sons, Inc. 1962).

[75] A. Cox, Lengths of geomagnetic polarity intervals, J. Geophys. Res. **73**, 3247-3260 (1968).

[76] N. O. Weiss, The expulsion of magnetic flux by eddies. Proc. Roy. Soc. A **293**, 310-328 (1966).